

27th April 2023

Dear Editor,

We are thankful for the possibility of reviewing our work for the EGU journal *Weather and Climate Dynamics*.

Some substantial modifications have been added with respect to the initial pre-print of the manuscript. While in-text revisions are provided in the marked-up version of the manuscript, we list some major changes in the points below. Please note that figures are referred to by their number in the manuscript revision.

- Following comment 1.3 by Reviewer #2, a new idealised experiment run with the SPEEDY model, featuring a Tibetan Plateau (TP) cooling only, was added to the previous Mongolian Plateau (MP) and MP+TP experiments. New panels relative to the TP experiment are now shown in **Figures 4, 7 and 8** and discussed in the **Results** section.
- Three new Figures and a revision of **Figure 7** are inserted and described in the manuscript to address issues raised by the Reviewers (for details see point-by-point answer below).
 - **Figure 1** shows the CMIP6 multi-model mean bias and the individual models' biases over the TP in terms of near-surface temperature.
 - **Figure 5** displays the mean sea-level pressure, 500 hPa geopotential height and 300 hPa zonal wind fields, which are useful to assert the strengthening of the East Asia winter monsoon.
 - **Figure 8** provides information on the upper-level eddy total energy flux (TEF). It is useful for understanding the propagation and intensity of the eddy energy over the Pacific and allows an intuitive interpretation of the changes in MEMF (RHS of Figure 7). The significance analysis is not applied to the results of this Figure.
 - The RHS panels of **Figure 7** have been revised to account for the significance analysis and for upper-level (instead of lower-level) changes in the synoptic variability. It now shows meridional eddy momentum flux at a pressure level of 300 hPa (MEMF, significant where stippling is shown) and its convergence (purple contours).

We have addressed all the Reviewers' comments and acknowledge major improvements in the manuscript thanks to the recommended changes. In the following we include the point-by-point answer to the comments and the marked-up version of the manuscript.

Kind regards,

Alice Portal (on behalf of the authors)

Note that line and figure numbers refer to the marked-up manuscript.

Reviewer #1

Based on the composites of CMIP6 models, this paper shows a cold bias over the Tibetan Plateau (TP), and finds that the negative temperature anomalies over TP intensify the East Asia winter monsoon by enhancing the low-level baroclinicity in the region of the East China Sea. Then, the southern flank of the Pacific jet is reinforced. The responses of AGCM experiments support the results of CMIP6 composite. Results are interesting and a cause for concern. The manuscript is generally well written and the methods appear sound. Since there are still some points need to be revised, I would like to recommend a moderate revision before this paper can be accepted for publication.

General comments:

1.1 Why exclude December from the analysis? The period of December-January-February is usually considered as the deep winter in East Asia, and December should be included in order to assess the full climatology of TP temperature and Pacific jet. In addition, for the climate conditions in Asian region, the January-February sometimes denotes the late-winter. The temperature variability and atmospheric climatology associated with the East Asian winter monsoon have obviously subseasonal variations (e.g., Zhong & Wu, 2022, <https://doi.org/10.1007/s00382-022-06610-9>; Park & Kim, 2021, <https://doi.org/10.1007/s00382-020-05544-4>; Tian & Fan, 2020, <https://doi.org/10.1007/s00382-019-05068-6>) from the early- to late-winter. So, if the cold TP bias and the related dynamic processes proposed in the study are also applicable in the early-winter (i.e., November-December)?

We agree with the reviewer's point. However, our analysis shows that the "cold-TP composite" anomalies in temperature and 850-hPa zonal wind (as shown by supporting Figures R1 and R2, here included) based on the periods "December-January-February" and "January-February" are almost indistinguishable. Because of this, and for consistency with the related Portal et al. 2022 (ref in the manuscript, using a similar experimental setup), we prefer to show the results in terms of January-February winters. Moreover, the choice of JF is not uncommon within the topic, e.g. see

Jhun, J., & Lee, E. (2004). A New East Asian Winter Monsoon Index and Associated Characteristics of the Winter Monsoon, *Journal of Climate*, 17(4), 711-726.

Clark, M. P. and Serreze, M. C.: Effects of variations in East Asian snow cover on modulating atmospheric circulation over the North Pacific Ocean, *Journal of Climate*, 13, 3700–3710, 2000.

We mention the similarity of JF and DJF results in Methods 2.1, **line 136**.

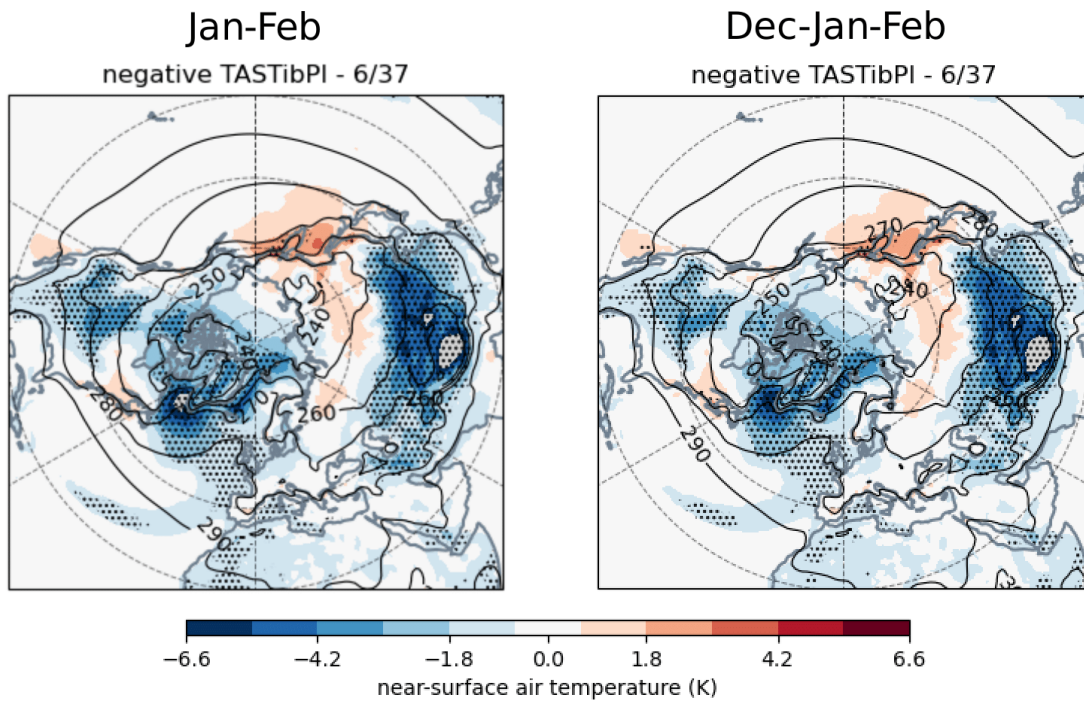


Figure R1: near-surface temperature anomaly in the “cold TP composite”, version JF (left) and DJF (right). Figure on the left is as Figure 2a from the manuscript.

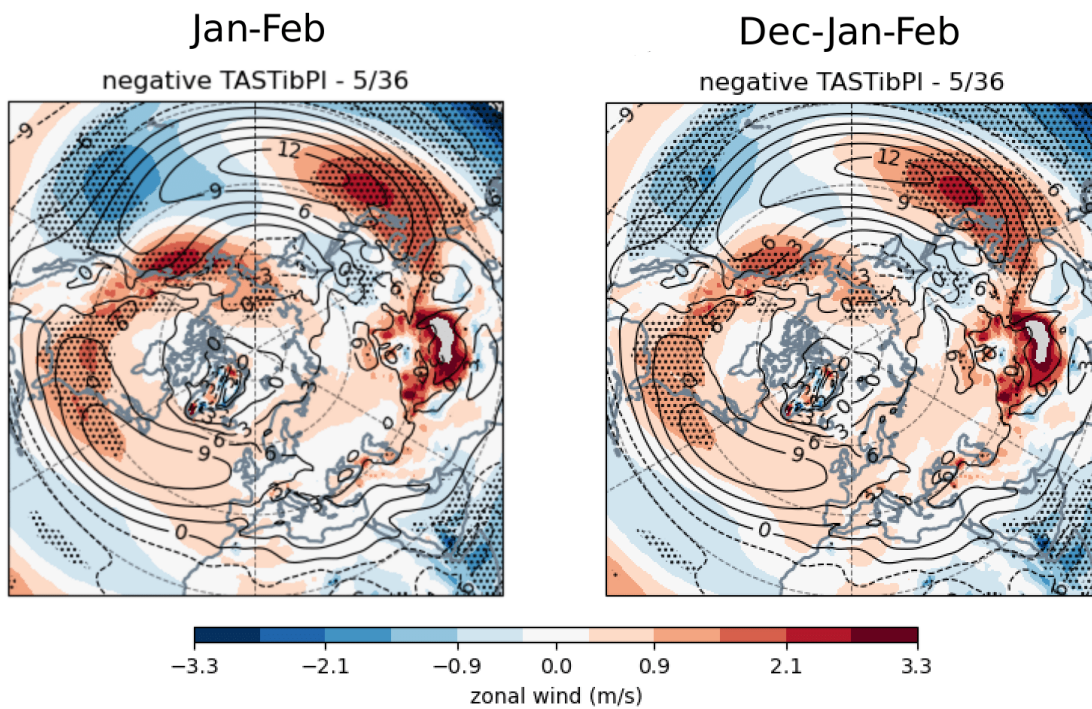


Figure R2: 850-hPa zonal-wind anomaly in the “cold TP composite”, version JF (left) and DJF (right). Figure on the left is as Figure 2c from the manuscript

1.2 Some model evaluations for the SPEEDY are needed, and at least one to be considered is the climatology of East Asian jet in AGCM and in CMIP6. Although the authors use the same surface temperature forcing as those in TP composite to drive the AGCM, the strength and position of cold advection and eddy growth rate are different (Figures 4 & 5). Compared to the CMIP6 composite, the temperature advection and eddy growth rate in AGCM are distributed farther east and closer to the Pacific and may contribute to less climate effects over the East Asian continent. Is the climatology of Asian jet in SPEEDY different from that in CMIP6 MME?

We thank Reviewer #1 for the interesting comment. Indeed, the 850 hPa zonal wind of the SPEEDY climatology and of the CMIP6 MMM are considerably different (see Figure R3 below): this is expected since SPEEDY is not a full-fledged atmospheric climate model, but relies on a simplified physics. Indeed, the eddy-driven jet in SPEEDY is weaker and shifted towards the north of the Pacific basin. However, in both cases the TP cooling affects the 850 hPa jet similarly over the East-Asian coast, with a weakening of the winds to the east of the orography. The limited eastward extension of the positive signal in the MMM (Figures 3(c) and 4(b)) is probably linked to other factors influencing the Pacific circulation within the cold TP composite (see e.g. the positive temperature advection in Figure 4(a) and surface latent heat flux Figure 2(c)) more than to differences in the mean state. We mention this shortcoming in the Results, **line 325**.

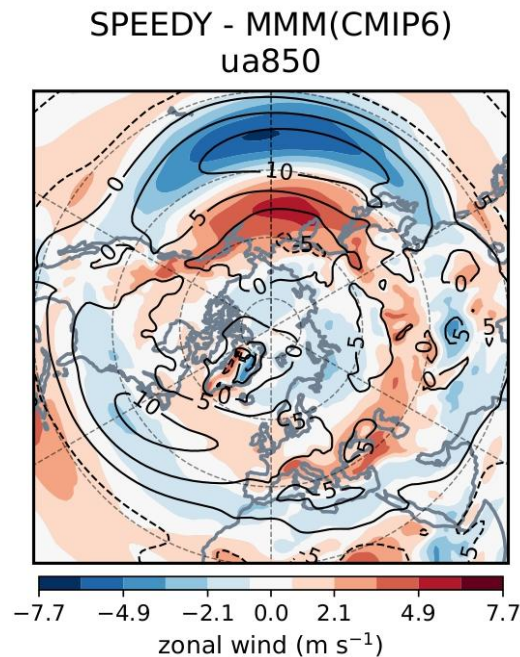


Figure R3: difference in Jan-Feb 850-hPa zonal wind between SPEEDY climatology and the CMIP6 multi-model mean (MMM). Contours denote the MMM isolines.

1.3 How does the cold TP bias construct in CMIP6 climate modes, snow cover over TP or other processes related to the surface heat fluxes? More discussions should be provided in the manuscript. Additionally, for the temperature advection, the authors only present the cold advection by the mean flow (i.e., Figure 4a). However, the anomalous low-level winds are also important to advect the surface temperature. How about the temperature advection by the anomalous winds?

The paragraph in **lines 104-116** has been inserted in the Introduction to provide a plausible explanation for the TP cold bias in terms of heat fluxes.

The temperature advection ($\mathbf{u} \cdot \nabla T$) is the dot-product between the velocity and the gradient vectors. Its anomaly from the climatological value takes into account the “cold composite” climatological anomalies from the MMM wind and temperature fields. This means that the temperature advection has not been expressed in terms of decomposition of the two linear terms (i.e. anomalous temperature advection by the MMM mean flow and MMM temperature advection by the anomalous flow).

1.4 In fact, the cold bias of winter temperature is not limited to TP, but the whole East Asia which is similar to those in CMIP5 models (e.g., Gong et al., 2014, <https://doi.org/10.1175/JCLI-D-13-00039.1>; Wei et al., 2014, <https://doi.org/10.1007/s00382-013-1929-z>). I suggest that the authors should give a brief discussion about the cold bias between CMIP5 and CMIP6 models.

We extend in the Introduction the discussion of East-Asia temperature biases throughout the recent CMIP phases following the advice of the Reviewer (**lines 90-99**). The suggested references are also mentioned in the Conclusions (**line 407**).

Furthermore, to better frame the discussion on the TP bias, **Figure 1**, showing the Northern Hemisphere MMM near-surface temperature bias (**a**) and the bias over the TP for each model (**b**), is also included in the revision.

Specific comments:

2.1 Suggest to change the title to reflect the East Asian winter monsoon. How about “Atmospheric responses in East Asia to wintertime Tibetan Plateau cold bias in CMIP6 models”?

Following the reviewer’s comment, the title has been changed to: “Atmospheric response to cold wintertime Tibetan Plateau conditions over East Asia in climate models”.

2.2 The physical processes associated with the atmospheric responses to the cold TP bias are in line with expectations and previous analyses as illustrated in Introduction (i.e., L42-L47). So the novelty of the study needs to be better explained given these works.

We add context to the statement of novelty of the study. We state that the cold TP forcing amplifies the atmospheric response to East-Asian orographic forcing shown by previous works (modifications in Abstract - **line 14**, Results - **lines 268-272**, Conclusions - **lines 386-389**).

2.3 Throughout the paper, words like the “bias” and “spread” are cross-used. They should have different meanings, and it’s better to define them more clearly in the paper.

We thank the reviewer for pointing this out. In the new version of the manuscript, we address this problem by using the two terms more accurately. This is helped by the addition of a **Figure 1** displaying CMIP6 near surface temperature bias.

2.4 “Cold bias” in your title should mean the temperature difference between the model simulation and observation. However, no observation data are used and the definition of “cold TP composite” in the paper does not meet the meaning of “bias”. I suggest a more appropriate word.

See answer to comment 2.3. The word “bias” has been removed from the title.

2.5 In Table 1, it would be more helpful to provide the latitude & longitude resolution in degrees or grid cells for each model.

The longitude x latitude grid spacing has been inserted in **Table 1**.

2.6 L187: Figure 2(b, d) may be Figure 3(b, d).

We thank the reviewer for the correction.

Reviewer #2

The authors present an interesting and sound analysis of the influence of cold biases in CMIP6 models/AGCM and its influence on the atmospheric state across east Asia and the North Pacific. The results presented by the authors is of interest and relevant to the journal, however I believe it could be improved by expanding on some results further and exploring model sensitivity. Furthermore, a greater explanation of the results from the SPEEDY model would be welcome. I list my several major points below as well as some more minor comments. Once these are addressed I see no reason why this manuscript should not be accepted for publication.

Major Comments

1.1 It would be beneficial to show some of the model spread in the cold bias. Several things that would improve the analysis are: is it only the cold models that have the downstream response in heat fluxes, wind biases, Eady growth rate, etc. A comparison of warm and cold models would be useful. Furthermore, all changes are expressed relative to the model mean, but are the models already biased relative to the observations/reanalysis? Do these cold models amplify an existing model mean bias or how much of the bias can be associated with the colder models? Do the coldest models have the largest biases in heat fluxes etc? I suggest plotting a scatter plot of temperature bias in the TP/MP region against average heat flux (or wind bias) downstream to test this.

The role of the CMIP6 TP cold bias has been further expanded in the new version of the manuscript. **Figure 1** now shows the bias in near-surface temperature, completing the information on the inter-model spread shown in **Figure 2a**. We have corrected the text in order to avoid confusion between the terms bias, spread and anomaly from the multi-model mean.

Furthermore, in Figure R4 (below) we report a scatter plot of TP near-surface temperature against surface sensible heat flux in a lon-lat box to the south of Japan. It shows a substantially linear relation between the near-surface temperature on the Tibetan Plateau and the downstream sensible heat flux (uw.), with correlation coefficient of -0.85 . confirming that the TP temperature plays a role in the downstream conditions generally among CMIP6 models, not only in the “cold TP composite”. We report this new result in the manuscript at **lines 294-301**.

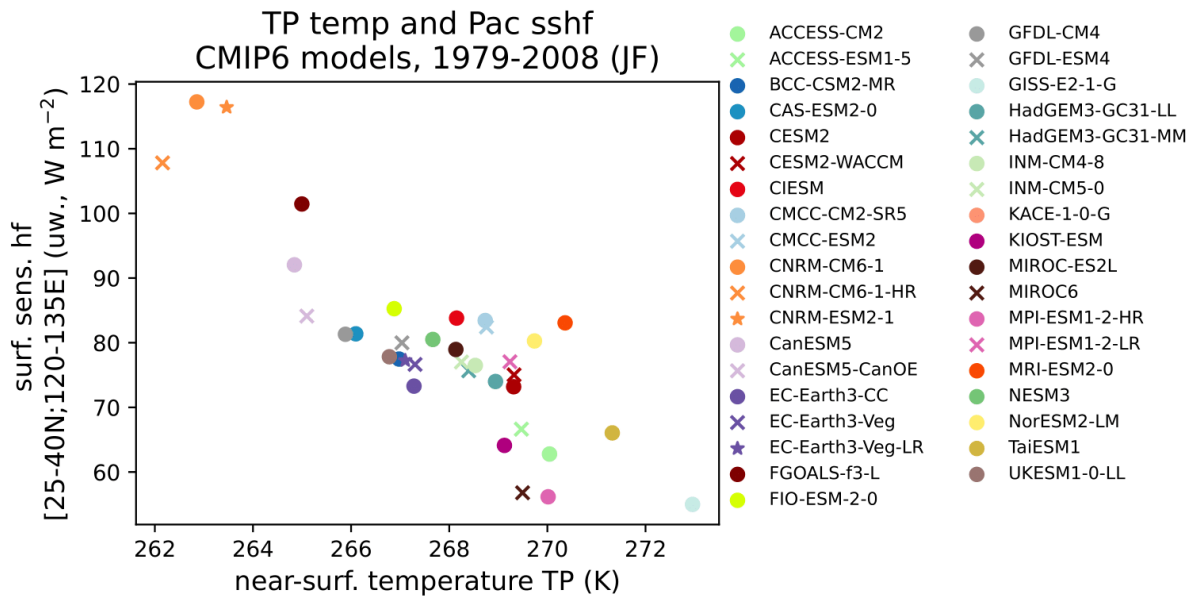


Figure R4: Scatter plot between TP near surface temperature (area-weighted average over lat-lon box [25-40N,70-105N]) and Pacific surface sensible heat fluxes south of Japan (area-weighted average over lat-lon box [25-40N,120-135N]).

1.2 What is the spread in response in the SPEEDY simulations? No stippling is shown in Fig. 5. I suggest something similar as above to investigate the variability in AGCM response.

The significance of the variables in SPEEDY has been computed and stippling has been added to **Figure 7** (former Fig 5).

1.3 You have performed a TP+MP and MP cold experiments and come to the conclusion that most of the downstream response is a result of the TP forcing. Surely running experiments of just the TP cold bias would answer this question. I suggest the authors address this in some way.

We are grateful to the reviewer for this suggestion, which elucidates further how the temperature in the TP region leads to a strengthening and southward shift of the downstream circulation. We included the description of the new TP forcing experiment in the Methods and its results in **Figures 4,7,8**, and expanded the corresponding discussion in the Results (**lines 364-373**) and Conclusion (**lines 396-404**).

Minor Comments

2.1 L37-38: I suggest adding a reference to Fig. 1b here.

The reference has been included.

2.2 L150: hyphen required in years.

The typo has been corrected.

2.3 L151 and Fig. 1a: how do you determine spread? Is this just the standard deviation of the temperature at each grid point?

We thank the reviewer for pointing out the missing information. In the Results section (**line 217**) and in the caption of **Figure 2**, we include text explaining that the spread is the standard deviation over the models' climatologies.

2.4 L154: incorrect colour labelling and figure reference – please correct.

Correction applied.

2.5 L167: 'land' not required.

Correction applied.

2.6 L180-185: suggest adding more explanation here on the mechanism as to how the cold TP bias influences the flow downstream. This will just need to add some discussion from the introduction I believe.

We expand on the reasons for jet strengthening in the paragraph at **lines 273-287**. Please note that the Figures have modified numbering in the new manuscript.

2.7 L188-189: suggest adding some lat/lon co-ordinates to reference which part of the Chinese coast line you are referring to – it's slightly confusing.

Latitude reference has been included.

2.8 Is there anything particular about the models that have the largest cold bias? Are they of lowest horizontal or vertical resolution?

Information about models' resolution has been included in **Table 1**, but no evident correlation exists between cold TP and resolution, suggesting that this might be part of the land-surface scheme.

Anonymous Referee #3

This paper investigated the atmospheric response to wintertime cold Tibetan Plateau (TP) bias with CMIP6 multi-model mean (MMM) simulations and idealized SPEEDY experiments. The authors found that the cold bias over Asian orography intensifies the East Asia winter monsoon (EAWM) through enhancing the low-level baroclinity and reinforcing the southern Pacific jet. The EAWM is a three-dimensional climate system and more details should be examined to measure its strength. Thus, I recommend a major and mandatory revision before the paper could be accepted. The details of the comments are listed below.

Major comments:

This study investigated the impacts of the cold bias over Asian orography on East Asia winter monsoon (EAWM). The EAWM is a three-dimensional climate system (e.g., Jhun et al. 2004) and its strength could not be simply measured by the wind at 850hPa. Thus, the authors should carefully check the atmospheric anomaly (e.g., Z500, U300, SLP) to measure the strength of EAWM (Jhun et al. 2004, Wang et al. 2010).

We agree with the reviewer's comment. **Figure 5** is added to the manuscript in order to detail the vertical structure of the EAWM. The consistency with East Asia winter monsoon strengthening, with reference to Jhun et al. 2004, is discussed in the Results **lines 264-272**. Moreover, in the SPEEDY experiments, we add in **Figures 7,8** and in the paragraphs from **line 330 to line 373** results regarding the upper-level storm track and its momentum deposition on the tropospheric jet.

Other comments:

2.1 Line 101: 'the January and February months are referred to as winter'. Why December is not considered? In general, the boreal winter is referred as "December-January- February" (DJF).

The results of the model compositing do not change if considering JF instead of DJF. See Figures R1 and R2 included below. This is mentioned in the Methods section, **line 136**.

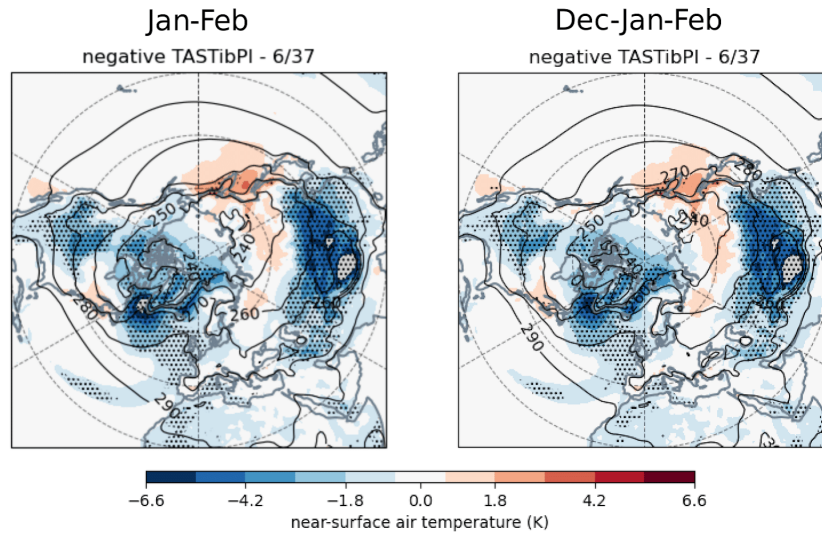


Figure R1: near-surface temperature anomaly in the “cold TP composite”, version JF (left) and DJF (right). Figure on the left is as Figure 2a from the manuscript.

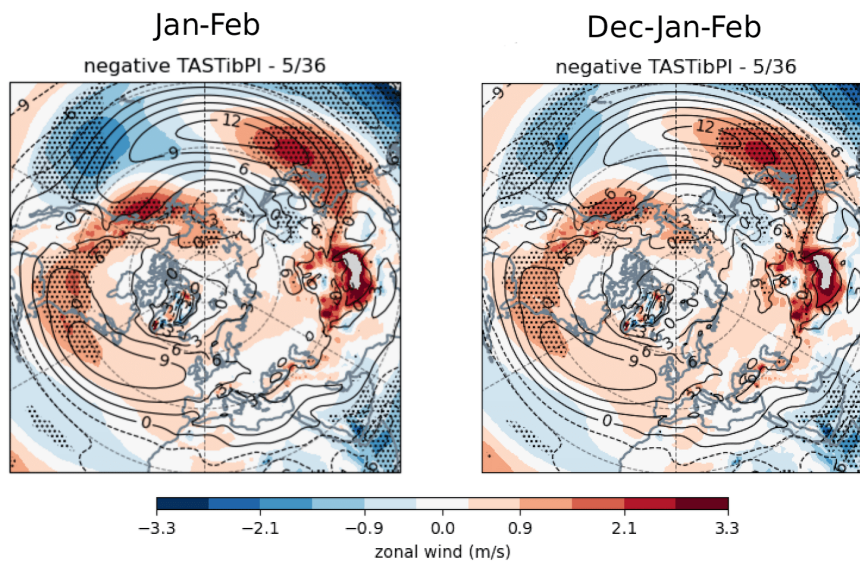


Figure R2: 850-hPa zonal-wind anomaly in the “cold TP composite”, version JF (left) and DJF (right). Figure on the left is as Figure 2c from the manuscript

2.2 Line 37: 40°N could be better.

Correction applied.

2.3 Line 128: As mentioned in line 125, the LST is prescribed in SPEEDY model. However, it is also proposed that the model includes a freely evolving LST scheme. I wonder how the LST is treated in the SPEEDY simulations? Could the LST be affected by upper-level circulation, or it is just prescribed as a model input? Please clarify.

The LST in the freely evolving versions interacts with the upper-level circulation by responding to a surface energy-balance equation, while relaxing towards a prescribed climatology - the relaxation time scale is 40 days. In the prescribed LST case (used here) the LST is simply fixed to the prescribed field, and does not evolve.

A detailed description of the LST scheme is available in Appendix B of

Portal, A., C. Pasquero, F. D'Andrea, P. Davini, M. E. Hamouda, and G. Rivière, 2022: Influence of Reduced Winter Land–Sea Contrast on the Midlatitude Atmospheric Circulation. *J. Climate*, **35**, 2637–2651, <https://doi.org/10.1175/JCLI-D-21-0941.1>.

Such reference is provided also in the Methods of the manuscript, section 2.2.

2.4 Line 150: '1979-2008' could be better.

The correction has been applied.

2.5 Figure 2: Please check the unit of the heat flux. It could be W m⁻².

Correct, we thank the reviewer for pointing out this mistake.

2.6 Figure 2: Positive value means upward or downward heat flux? Please provide the information in figure captions.

It is an upward heat flux. The issue has been addressed.

2.7 Line 170: The statement could be misleading. The heat flux change is negative over TP regions.

We specify in the description (Results) that enhanced cooling is present where the turbulent heat fluxes are climatologically negative, **lines 240-242**.

2.8 Line 171: If the heat flux change is not significant over TP and CP, why the authors show the heat flux change here? It could confuse the readers.

From **Figure 3b,c** we note that stippling (significant signal) is present over the TP and the MP, even if it does not extend uniformly over the entire region. We clarify the confusion in **lines 242-243**.

2.9 Line 184: The jet stream distributes around 300hPa during winter (Jhun et al. 2004). The statement here could be misleading.

We now specify that in this context we are referring to the eddy-driven jet.

2.10 Line 187: Please check the figure captions.

The caption has been corrected.

2.11 Line 190: Increased instability favors acceleration of upper-level zonal winds (e.g., Nie et al., 2016). Please show the zonal wind change of upper troposphere.

The upper-level jet is now shown in the **Figure 5(c)** and the analysis of eddy momentum deposition in the SPEEDY experiment is also shown for the upper troposphere (**Figures 7,8**).

2.12 Line 214: Please check the figure captions.

The caption has been revised.

2.13 Figure 5: Please show the significant information of the changes as in Figure 4.

Stippling to indicate the significant changes has been included in the updated figure.

2.14 Line 199: Please show the surface wind anomaly with vectors. Otherwise, one may not understand the heat flux anomaly.

Following the reviewer's comments, we have inserted in **Figure 3c** vectors showing significant wind anomalies at 1000 hPa (near-surface wind was unavailable for ~10 models, hence the 1000 hpa pressure level was preferred).

2.15 Line 200: More upward heat flux? Please clarify.

The sentence has been rephrased.

Reference:

Wang, B., Wu, Z., Chang, C., Liu, J., Li, J., & Zhou, T. (2010). Another Look at Interannual-to-Interdecadal Variations of the East Asian Winter Monsoon: The Northern and Southern Temperature Modes, *Journal of Climate*, 23(6), 1495-1512.

Atmospheric response to cold wintertime Tibetan Plateau ~~cold bias~~ conditions over East Asia in climate models

Alice Portal^{1,2}, Fabio D'Andrea², Paolo Davini³, Mostafa E. Hamouda^{4,5}, and Claudia Pasquero^{1,3}

¹Department of Earth and Environmental Sciences, Università di Milano - Bicocca, Milan, Italy

²Laboratoire de Météorologie Dynamique/IPSL, École Normale Supérieure, PSL Research University, Sorbonne Université, École Polytechnique, IP Paris, CNRS, Paris, France

³Consiglio Nazionale delle Ricerche, Istituto di Scienze dell'Atmosfera e del Clima (CNR-ISAC), Torino, Italy

⁴Astronomy and Meteorology Department, Faculty of Science, Cairo University, Cairo, Egypt

⁵Institute for Atmospheric and Environmental Sciences, Goethe University Frankfurt, Frankfurt am Main, Germany

Correspondence: Alice Portal (a.portal@campus.unimib.it)

Abstract. Central Asia orography (namely the Tibetan and Mongolian plateaux) sets important features of the winter climate over East Asia and the Pacific. By deflecting the mid-latitude jet polewards it contributes to the formation of the Siberian High and, on the lee side, to the advection of dry cold continental air over the East Asian coast and the Pacific Ocean, where atmospheric instability and cyclogenesis thrive. While the ~~mechanical~~ mechanic forcing by the orography is assessed ~~by~~ in a number of modelling studies, it is still not clear how near-surface temperature over the two most prominent orographic barriers of the Central Asian continent ~~, namely~~ the Tibetan and Mongolian plateaux ~~,~~ influences the winter climate ~~downstream~~. ~~Moreover,~~ The problem is particularly relevant in view of a well known ~~issue of cold bias in~~ state-of-the-art climate models ~~is a cold land temperature bias over in proximity of~~ the Tibetan Plateau, likely related with the ~~difficulty in modelling~~ modelling of land processes and land-atmosphere interaction over complex orography. Here we take advantage of the large spread in ~~representing near-surface~~ near-surface temperature over the Central Asia plateaux ~~among climate models taking part in within~~ the Coupled Model Inter-comparison Project, Phase 6 (CMIP6) to study how ~~temperatures over these regions colder than average~~ Asian plateau temperatures impact the atmospheric circulation. Based on composites of the CMIP6 models' climatologies showing ~~a cold bias over the Tibetan Plateau coldest Tibetan Plateau conditions~~, we find that such negative temperature anomalies ~~over Asian orography intensify the East Asia~~ amplify the atmospheric response to orography, causing an intensification of the East Asian winter monsoon and ~~, by enhancing the low-level baroclinicity in the region of the East China Sea, reinforce the southern of the equatorward~~ flank of the Pacific jet. The results of the CMIP6 composite analysis are supported by ~~the response of experiments run with~~ an intermediate-complexity atmospheric model ~~to~~ and forced by a similar pattern of cold surface temperatures over the Central Asia plateaux; ~~we also distinguish~~. Within this setting, the relative influence of the Tibetan and the Mongolian Plateau surface conditions ~~, thereby, based on the intensification of the East Asia winter monsoon in models characterised by a cold land temperature (bias) over Central Asia plateaux, is analysed. Based on the results reported in this work~~ we prospect that advances in the modelling of the land energy budget over ~~this region may the elevated regions of Central Asia could~~ improve the simulation of the ~~mean climate over the~~ East Asia / Pacific sector climate, together with the reliability of climate projections and the performance of shorter term forecasts.

Short non-technical summary. The differences between climate models can be exploited to infer how specific aspects of the climate influence the whole Earth system. This work analyses the effects of a negative temperature anomaly over the Tibetan Plateau and its surroundings on the winter atmospheric circulation. We show that models with a colder-than-average Tibetan Plateau present a ~~reinforced East Asia~~ reinforcement of the East Asian winter monsoon and we discuss the atmospheric response to the enhanced transport of cold air from the continent toward the Pacific Ocean.

1 Introduction

The impact of orography on the extratropical circulation was proposed by the analytical studies of Charney and Eliassen (1949) and Bolin (1950), while Smagorinsky (1953) first discussed the matching of orographic and thermal forcing by land-sea contrast in order to explain the longitudinal variations of the mid-latitude westerlies. Manabe and Terpstra (1974) and Hahn and Manabe (1975) analysed the impact of the Tibetan Plateau on the Asian climate by running an atmospheric general circulation model (AGCM) with and without mountains. They proved that the elevation of ~~central~~ Central Asia is essential to reproduce the position and strength of the low-level winter anticyclone known as the Siberian High and for the maintenance of the South-East ~~Asia~~ Asian summer monsoon, which, ~~due thanks~~ to the intense uplift from orography, extends from the Indian sector as far as East Asia. The regional dryness and humidity of the aforementioned winter and summer circulation patterns and their association with orography were examined by Broccoli and Manabe (1992).

More recently, starting with Sato (2009), the influence of ~~lower-range~~ lower elevation mountain chains on the Asia and Pacific climate ~~was investigated, and their role was~~ has been considered separately from that of the Tibetan Plateau. This applies in particular to the mountain chains extending north east of Tibet. Similarly to White et al. (2017), we denote the orography between approximately 20 to 40°N and 62 to 120°E as the Tibetan Plateau or TP region (green box in Figure 2), and that between approximately 38 to 60°N and 65 to 140°E as the Mongolian Plateau or MP region (orange box in Figure 2).

In the cold season the East Asia / Pacific circulation is dominated by the East ~~Asia~~ Asian winter monsoon, which consists in north-westerly advection of cold dry continental air from Siberia ~~over off~~ the Asian coast ~~and the Pacific Ocean~~ (Zhang et al., 1997; Chan and Li, 2004). The ~~strong~~ winter thermal emission of the TP land and of the air column above generate a tropospheric heat sink over the Plateau (Yanai et al., 1992; Yanai and Wu, 2006; Duan and Wu, 2008) that reinforces the Eurasian mid-tropospheric thermal high (Shi et al., 2015). Moreover, the presence of TP and MP orography reduces the westerlies upstream and enhances the north-westerly winds over East Asia and the Pacific (Shi et al., 2015; Sha et al., 2015). On the lee side of the plateaux, the cold ~~advection strengthens the thermal contrasts and increases the~~ continental advection modulates the thermal contrast with the Pacific Ocean and the local baroclinicity, which ~~in turn fuels~~ fuel the Pacific jet stream downstream ~~, over and east of the East China Sea~~ (Shi et al., 2015; White et al., 2017). Notwithstanding the lower elevation and extension of the MP compared to the TP, the MP is more relevant for the winter circulation because of its ideal position - in terms of impinging low-level winds and meridional potential vorticity gradients - for acting as a source of Rossby waves (Held and Ting, 1990; White et al., 2017).

Conversely, the warm season circulation is driven by the East ~~Asia-Asian~~ summer monsoon, modulating rainfall over land and ocean (Yihui and Chan, 2005). This is sustained in strength and extension by the atmospheric uplift produced by ~~Asia Asian~~ orography, which constitutes a tropospheric ~~summer heat source~~ heat source in summer (Yanai et al., 1992; Hahn and Manabe, 1975; Ye and Wu, 1998). The orographic control over the summer monsoon is mostly ~~controlled by the presence of~~ the-TP-accomplished by the TP - the MP playing only a marginal role - which, among other things, reinforces the monsoonal circulation and the associated precipitation along the east coast of Asia ~~-, with the MP playing only a marginal role-~~ (see Figures 6, 9, 10 in Sha et al., 2015).

Considering the importance of the Central ~~Asia-Asian~~ orography for the climate of the Asia / Pacific sector, it is not surprising to find examples in literature where orographic surface and near-surface ~~conditions (contributing to the tropospheric heat sources or sinks, Y~~ thermal conditions (acting as tropospheric heat sources or sinks, Yanai et al., 1992) have an impact on the ~~atmospheric conditions~~ circulation downstream. Indeed, evidence is found ~~on-for~~ the relevance of spring and summer temperatures over Asian orography for the ~~successive~~ atmospheric conditions far downstream (see Wu et al. (2015) for a review and Xue et al. (2021, 2022) for recent work on the impact of spring TP land initialisation in subseasonal-to-seasonal predictions). In the extended winter season (October–March) the presence of anomalous snow cover changes the tropospheric energy budget through an increase of the surface albedo, enhancing the reflection of shortwave radiation and the cooling of the land surface and the atmosphere (Yeh et al., 1983). Analyses on the dynamical influence of Tibetan Plateau snow cover indicate that it is relevant for the atmospheric circulation at intraseasonal time scales (Li et al., 2018) and that, when anomalies are persistent, it ~~can may~~ modulate interannual variability (~~Chen et al., 2021; Clark and Serreze, 2000~~) (Chen et al., 2021; Clark and Serreze, 2000; Henderson et al., 2013) and long-term projections (Liu et al., 2021). ~~Contrarily to the extensively discussed impact of autumn Siberian snow cover on the winter circulation (e.g. Cohen et al., 2014; Garfinkel et al., 2010; Henderson et al., 2018), the dynamical role of anomalous surface conditions over the Tibetan and Mongolian plateaux has been poorly investigated, notwithstanding its potentially high impact on East Asia.~~ In a more idealised context, winter positive thermal forcing over mid-latitude land - as in a climate with a reduced winter land-sea thermal contrast caused by the faster warming of continents with respect to oceans - was analysed by Portal et al. (2022). It was ~~there shown~~ shown there that the atmospheric response to idealised warming over East Asia (including the orography) dominated over a pattern of similar intensity imposed ~~in North America~~ over the North American continent. The work by Henderson et al. (2013), comparing snow-induced temperature forcing over the two continents, reaches similar conclusions regarding the relevance of East Asian surface conditions for the Pacific sector. A possible explanation for this is that ~~-, because the high orographic elevation of the Asian forcings acts as a heat source directly in the~~ elevated Asian forcing, heating directly the mid troposphere, ~~it was is~~ more effective in producing a large hemispheric response than ~~the equivalent low-level~~ an equivalent lower-level forcing over the North ~~American continent (Hoskins and Karoly, 1981; Trenberth, 1983; Ting, 1991).~~ America (Hoskins and Karoly, 1981; Trenberth, 1983; Ting, 1991). Notwithstanding the potentially high impact of anomalous surface conditions over the Tibetan and Mongolian plateaux on the East Asian climate, their dynamical role has been poorly investigated.

~~Recently, output from the CMIP6 showed~~ An additional motivation to approach the topic of thermal forcing over the Asian plateaux is the presence of a significant multi-model mean (MMM) temperature bias in the region of ~~the-TP-East Asia,~~

which is evident over successive phases of the CMIP and over multiple seasons. Priestley et al. (2022) detect a strong deviation from the reanalysis ~~for summer temperature~~ temperature in the summer season and, based on the modified thermal gradients in the ~~low-lower~~ troposphere, hypothesise a role of the TP land temperature on the baroclinicity and cyclogenesis downstream. Along the same lines, ~~Peng et al. (2022) and Fan et al. (2020) find a cold TP bias in winter for the MMM~~
95 ~~near-surface temperatures; the improvements~~ East Asian winter conditions are anomalously cold among several climate models (Wei et al., 2014; Gong et al., 2014), although improvements, associated with a closer representation of the winter monsoon, have been detected in the transition from ~~Phase 5 to Phase 6 of the CMIP are limited~~ CMIP Phase 3 to Phase 5 (Wei et al., 2014). The winter bias is specially strong over the TP region (Figure 1 and Peng et al., 2022; Fan et al., 2020), where limited progress was obtained in the transition from CMIP5 to CMIP6 (Lun et al., 2021; Hu et al., 2022). These ~~last~~ studies also highlight
100 the presence of a wide inter-model spread in year-round East Asian and TP temperatures among the ~~CMIP6~~ CMIP climate models, which ~~comes~~ appears to be related with the difficulties in representing surface energy fluxes ~~over complex orography~~ characterised by (Wei et al., 2014), in particular over regions characterised by complex orography and seasonal variations in snow cover (e.g. Su et al., 2013; Chen et al., 2017; Li et al., 2021).

~~Although the reason for the emergence of the~~ The cold Tibetan Plateau temperature bias ~~in many state-of-the-art climate~~
105 ~~models has been examined in some detail by Chen et al. (2017). Among the climate models taking part in CMIP5 they is examined in some detail by Chen et al. (2017),~~ identify a strong bias in the western region of the Plateau (consistent with Figure 1(a) and show that it is more evident in terms of near-surface than surface (skin) temperature. The reason for the emergence of the strong near-surface bias is investigated by decomposing the different contributions to the low-level energy budget. Anomalous snow cover corresponds to an increase in the surface albedo, hence in the reflection of shortwave radiation, and this is anti-correlated with upward turbulent heat fluxes. While the surface temperature is weakly affected by these terms, due to compensation between incoming shortwave radiative and outgoing turbulent fluxes, a reduction in the turbulent heat flux into the atmosphere, leading to a decrease in the low-level water vapour content and thermal radiation, cools the boundary layer. By identifying physically interlinked low-level and surface processes modifying the energy budget, Chen et al. (2017) are able to explain why several CMIP5 models present a low-level cold bias over the Tibetan Plateau. These
110 findings are likely applicable to the ~~dynamical consequences of~~ CMIP6 models affected by similar TP temperature biases (Lun et al., 2021; Hu et al., 2022).

~~In the present paper, by analysing~~ the ~~cold bias are yet to be explored. Hence, the aim of the present paper is to analyse~~
~~the~~ implications of cold Central Asia orography winter conditions ~~on for~~ the large-scale circulation on the lee side of the mountains, the possible dynamical consequences of the climate models' cold bias are explored. To do this we take advantage
120 of the large temperature spread detected over TP and MP among CMIP6 models to construct a multi-model realisation of ~~the cold bias (the a cold anomaly. The atmospheric circulation in such "cold TP composite"), over which we conduct an analysis of the Pacific sector atmospheric circulation, more specifically of the East Asia winter monsoonal circulation is analysed in the Asia / Pacific sector, taking into account the East Asian winter monsoon.~~ The results obtained from the multi-model study are further tested with an intermediate-complexity Atmospheric General Circulation Model (AGCM) forced by land-surface
125 temperature patterns ~~similar to the~~ taken from the anomalies in the CMIP6 "cold TP composite". Finally, to ~~shed light on the~~

isolate the individual role of the Mongolian Plateau and Tibetan plateaux in the atmospheric response to cold ~~land-over~~ Central Asia orography, we consider ~~a separate AGCM experiment where MP forcing is opposed to two separate AGCM experiments where MP or TP forcing are compared against~~ a widespread TP and MP forcing.

The two approaches (CMIP6 compositing and AGCM idealised simulations) are described in the Methods, the outcomes and their mutual consistency are examined and discussed in the Results and a final summary ~~and discussion considering previous literature~~ is provided in the Conclusions.

2 Methods

2.1 CMIP6 simulations

We use CMIP6 historical runs for years 1979–2008 and we compute the January–February climatology over the whole period; ~~the January and February months are~~ January–February is referred to as *winter* throughout the paper. ~~As in Clark and Serreze (2000) the~~ The results are equivalent for December–January–February winters, while, as in Clark and Serreze (2000), results for an extended winter taking into account the transition months (e.g. October–March) are weaker in intensity ~~;~~ ~~hence are not reported~~ (not shown). We select one member per climate model from the CMIP6 dataset, as specified in Table 1, giving a sample of 37 historical simulations. Based on an index of Tibetan Plateau temperature (i.e. the climatological weighted-area average ~~on of~~ near-surface temperature in the black box of Figure 2(b), comprising latitudes 25 to 40 N and longitudes 70 to 105 E over the period 1979–2008), the six simulations with temperature below one standard deviation from the CMIP6 multi-model mean (MMM) form the “cold TP composite” (see models highlighted in bold in Table 1). The composite fields are shown in terms of the anomalies from the climatology of the ~~CMIP6 multi-model mean (MMM), with significance computed according to a permutation test repeated~~ MMM, with stippling where the anomalies exceed the 95th percentile of a random distribution, computed from 1000 times over samples of 6-model composites extracted randomly and without repetition from the 37 model realisations ~~;~~ ~~considering the 95% confidence level (Wilks, 2011).~~ (Wilks, 2011). Stippled anomalies (as defined above) are referred to as significant within the text. Note from Table 1 that in the “cold TP composite” multiple models from the same institutions are chosen; the same selection, but based on a single model per institution, produces similar results (not reported).

Wind components and air temperature at levels between 1000 and 700 hPa–hPa and at 300 hPa are extracted from the CMIP6 archive and used in the analysis. Turbulent surface heat fluxes, surface temperature (skin temperature or SST for open ocean) and near-surface temperature (usually 2-meter air temperature) are also used. Due to the lack of availability of daily ~~frequency~~ condensed-averaged fields for a large subset of the CMIP6 models, the analyses on the “cold TP composite” are based on monthly-mean variables ~~condensed-averaged~~ in model climatologies. Moreover, we report that surface latent heat flux in KIOST-ESM, meridional wind and temperature advection in CAS-ESM2-0, zonal wind, temperature advection and Eady growth rate in FGOALS-f3-L are excluded from the analysis because of the inaccessibility of ~~some datasets from~~ the datasets in the servers providing the CMIP6 archive.

2.2 Idealised experiments

To confirm the ~~causal-link-between~~link between temperature and circulation anomalies in the results obtained from compositing on CMIP6 models we run idealised experiments using an 8-level AGCM developed at the International Centre for Theoretical Physics (ICTP), ~~and~~known as SPEEDY for Simplified Parametrization, primitivE-Equation DYnamics. The model is spectral on the sphere, with triangular truncation at total wavenumber 30 (T30) and a Gaussian grid of 96 by 48 points, and includes simple parametrisation of moist processes (Molteni, 2003). Despite the low horizontal and vertical resolution, SPEEDY displays an adequate performance for the analysis of large-scale features of the climate system (Kucharski et al., 2006, 2013). SPEEDY is run in perpetual-winter mode (200 January months and 200 February months) with prescribed sea-surface temperatures (SSTs), sea-ice cover (SIC) and land-surface temperatures (LSTs). Two ~~type-types~~of simulations are considered:

- a *control integration* where SST and SIC are equal to the 1979–2008 HadISST climatologies (Rayner et al., 2003). The LST corresponds to the climatology obtained from a SPEEDY ~~ensemble-10-member ensemble~~, run with a freely evolving LST scheme and with prescribed climatological SIC and evolving SSTs 1979–2008 from HadISST. Details on SPEEDY’s LST scheme are available in the Appendix B of Portal et al. (2022);
- ~~two-three~~cold integrations with SST and SIC as in the *control*, and with LST forcing corresponding to the significant ~~anomaly-anomalies~~ of surface temperature from the “cold TP composite” within 60–140 E and 20–60 N (“TP+MP experiment”) or within 60–140 E and 38–60 N (“MP experiment”) ;or within 60–140 E and 20–38 N (“TP experiment”), smoothed by $\exp\{-1/2 \cdot (5 \text{ lat})^2\}$ north of 38 N, interpolated onto SPEEDY’s grid (Figure 4(a,e,i)).

The responses ~~of-to~~“TP+MP” and, ~~“MP” forcing and~~“TP” forcing experiments visualised in the Results correspond to the climatological difference ~~“coldintegration - controlintegration”~~-, averaged over January and February. The stippling indicates anomalies exceeding the 95th percentile of a distribution obtained for each experiment by randomly permuting 1000 times the pool of daily fields composing the “cold” and “control” integrations. The fields are distinguished by month but not by forcing, in order to obtain 1000 realisations of the average January-February “(cold - control)_{perm}” anomaly (Wilks 2011). Stippled anomalies (as defined above) are referred to as significant within the text.

2.3 Diagnostics

We introduce ~~some-here the~~diagnostics used in the analysis of the results:-;

- ~~Temperature-temperature~~ advection is

$$-\mathbf{u} \cdot \nabla T = -\left(u \frac{\partial T}{\partial x} + v \frac{\partial T}{\partial y}\right),$$

where $\mathbf{u} = u\hat{\mathbf{i}} + v\hat{\mathbf{j}}$ is the horizontal wind composed ~~by-the-zonal-of the zonal u and meridional v components and meridional component and~~ T is the temperature:-;

– ~~The the~~ Eady growth rate corresponds to

$$\sigma = 0.31 f \frac{du}{dz} \mathcal{N}^{-1},$$

190 where f is the Coriolis parameter, z is the geopotential height and $\mathcal{N} \equiv \sqrt{(g/\theta) d\theta/dz}$ is the Brunt-Väisälä frequency with θ potential temperature and g Earth’s gravitational acceleration.

– ~~The~~

Both quantities are computed using mean climatological variables, giving the temperature advection by the mean flow and the Eady growth rate of the mean state.

195 The following diagnostics are computed for SPEEDY integrations only:

– meridional eddy momentum flux (MEMF) ~~is~~, the product of the 2–6 day Fourier filtered wind components $u^{\text{HF}} v^{\text{HF}}$. Its meridional convergence ($-\frac{\partial}{\partial y} (u^{\text{HF}} v^{\text{HF}})$) represents the dominant term of eddy momentum deposition in the zonal flow (Hoskins et al., 1983);

– eddy total energy flux (TEF, Drouard et al., 2015), used to estimate the downstream propagation of eddy total energy, and defined as

200

$$\text{TEF} \equiv \mathbf{u} \cdot (\text{EKE} + \text{EAPE}) + \mathbf{u}_a^{\text{HF}} Z^{\text{HF}}, \quad \mathbf{u}_a \equiv \mathbf{u} - \frac{g\hat{\mathbf{k}}}{f} \times \nabla z.$$

The contributions come from the advective flux of $\text{EKE} \equiv (\mathbf{u}^{\text{HF}})^2/2$ (eddy kinetic energy) and of $\text{EAPE} \equiv (h^2/s^2)(\theta^{\text{HF}})^2/2$ (eddy available potential energy)¹, and from the ageostrophic geopotential flux. The latter is defined in terms of z (geopotential height) and \mathbf{u}_a (ageostrophic horizontal wind).

205 ~~Among these, the temperature advection and the Eady growth rate are computed using mean climatological variables, giving the temperature advection by the mean flow and the Eady growth rate of the mean state. The climatological MEMF is~~ The climatological MEMF and TEF are computed on high-pass filtered daily fields (represented with superscript ^{HF}), averaged over the total time span of the model simulations duration of the SPEEDY integrations.

3 Results

210 The representation of the winter (January-February) near-surface ~~temperatures~~ temperature climatology by CMIP6 models in the historical period ~~1979-2008 shows a strong~~ 1979–2008 shows a cold bias over the Arctic and over many inland regions of the Northern Hemisphere, including most of East Asia, with a peak in the mid-west of the Tibetan Plateau (Figure 1(a)). Panel (b) of Figure 1 shows the average bias in the TP box (black box in Figure 2(b)) for each of the CMIP6 models: apart from

¹The EAPE parameters $s^2 = -h \partial \theta_c / \partial p$ and $h = (R/p)(p/p_s)^{R/C_p}$ depend on pressure (R is the gas constant, p_s is 1000 hPa, C_p is the specific heat of the air at constant pressure).

a few exceptions, models are colder than the reanalysis, and those belonging to the same institutions show consistent values. Otherwise, warm biases are detected in the entrance regions of the storm tracks, over north-east Siberia, in some areas of the Middle East, in the far-west (Hindu Kush) and far south-east (Hengduan Mountains) of the Tibetan Plateau.

The amplitude of the inter-model spread (in near-surface temperature (computed in terms of standard deviation) is displayed in Figure 2(a)). The spread generally is generally larger over land than over ocean and grows with latitude: the largest. Largest amplitude is attained around and poleward of the 60° N latitude circle, with a while the maximum over the Atlantic and Pacific Oceans is likely due to the inter-model variability in the position of the winter sea-ice cover boundary. An additional mid-latitude hot-spot can be easily identified in the mid-latitude continents over the Tibetan Plateau Tibetan Plateau, extending north to the Mongolian Plateau (cf. temperature spread and green /yellow and orange boxes over orography in Figure 2(a,b)). Since the atmospheric response to deep mid-latitude heat sources or sinks is specially strong (Trenberth, 1983), and, on top of likely in relation to this, the winter mid-latitude circulation is known to be highly sensitive to East Asia surface conditions (e.g. Portal et al., 2022; Cohen et al., 2001), Asian surface conditions (e.g. Portal et al., 2022; Henderson et al., 2013; Cohen et al., 2001), we analyse in the following we study the dynamical features of a “cold TP composite” obtained by averaging over. The composite is computed by averaging on a model selection based on a TP temperature index (see). The index (one value per CMIP6 model) is, corresponding to the area-weighted spatial and temporal average mean of near-surface temperature over the black box in Figure 2(b), a region characterised by large temperature spread and high elevation within the Tibetan Plateau domain (black box). The biases of the TP temperature indices with respect to reanalysis are displayed in Figure 21(b)).

Some relevant surface variables from the “cold TP composite” are presented in Figure 3. The near-surface temperature map features an intense cold anomaly on over the orography of Central Asia, peaking over the TP and extending north-eastwards to the MP. Significant We note that significant surface anomalies are also found found also elsewhere in the North America / North Atlantic sector (not shown), but, since the however, since our focus is on Asian orography and its downstream impacts, regional surface signals that are unlikely to interact with the Asia / Pacific sector are not neither presented nor discussed. By comparing the surface and near-surface temperature patterns over the TP (cf. Figure 4(a) and Figure 3(a)), we notice that the land-surface surface temperature anomaly is stronger in intensity than the near-surface anomaly, and conclude that in the “cold TP composite” , as described by Chen et al. (2017), land has a cooling effect on the atmosphere above. This feature is corroborated by negative anomalies of surface sensible and latent heat flux in a region. In regions where the MMM fluxes are -on average - weakly positive (Figure 3(b,e)), representing weakly positive this corresponds to a reduced latent and sensible warming of the atmosphere by the land surface . The in the cold composite models, where the MMM fluxes are negative it corresponds to enhanced atmospheric cooling by the surface (Figure 3(b,c)). The significant signal in sensible heat flux is strong over the center of the TP, while the latent heat flux term is significant elsewhere over the TP and MP regions.

In the “cold TP composite” anomalous snow amount is detected in correspondence of with the strongest sensible heat flux anomalies (not shown), but, since the anomalies are not significant, this is unlikely to explain by its own the surface temperature pattern. Chen et al. (2017) decompose the surface energy budget, but is not reported because data is available only for a limited sub-group of models. Although here we cannot verify the role of snow in the low-level energy budget, the anomalies in the surface variables are coherent with each other and with the results in Chen et al. (2017). They show that over the TP and

show that the TP processes causing cold biases are physically interlinked, involving anomalous snow cover may involve anomalous snow enhancing the surface albedo with negative effects on the low-level water vapor content and the downward longwave radiation, which ultimately result in a cooling of the surface boundary layer. The existence in CMIP6 models of a variety of schemes for land, snow and atmospheric boundary layer and of the mutual interaction between these over complex orography, is are likely at the origin of the wide inter-model spread. Furthermore, based on the results of Figure 4 and of Liu et al. (2022), the over the TP. In support of this view, the surface temperature anomalies do not appear to be driven by the circulation upstream of the TP (Figure 4 and 5).

The low-level temperature and wind conditions of the CMIP6 “cold TP composite” at 850 hPa are shown in Figure 4(a–d). We note that at 850 hPa the negative thermal anomaly is shifted north eastward extends north-eastward of the most elevated area of the Tibetan Plateau - represented by grey patching - and reinforces the thermal cooling induced by the uplift over MP orography, shown in Figure 11 of Sha et al. (2015) (cf. to Figure 11 in Sha et al., 2015). East of this region the westerly zonal winds (i.e. Pacific jet) are reinforced of the Pacific eddy-driven jet are reinforced (Figure 4(c)). At the same time, southward wind the southward wind anomaly over East China and northward wind and the northward wind anomaly over the Pacific ocean (Figure 4(d)) intensify the cyclonic circulation over the ocean give rise to a cyclonic anomaly over the Asian coast and reinforce the East Asia consequently also the East Asian winter monsoon.

Typical features relating to a strong East Asian winter monsoon are captured by the sea-level pressure and mid-troposphere geopotential height fields in Figure 5, as by comparing with strong and weak monsoon conditions in Figure 6 of Jhun and Lee (2004). A deeper zonal pressure contrast to the east of the Siberian High (Figure 5(a)) and a lower 500 hPa isobaric surface over the Asian coast (Figure 5(b)) reinforce the 300 hPa jet over land and south of Japan (Figure 5(c)), and adhere to maps describing the atmospheric state associated with an intense monsoon. A further comparison with the maps in Sha et al. (2015) and Shi et al. (2015) shows that the cooling over Central Asia orography amplifies the atmospheric response to orography itself. The positive interference between orographic forcing and superposed cooling corresponds closely to the outcome of a set of idealised experiments by Ringler and Cook (1999), featuring combinations of mechanic orographic and thermal forcing under varying mean-flow conditions.

The advection of cold air downstream of the TP (Figure 6(a), see for details on the computation) is supported both by the negative temperature anomaly on the orography and, to the east, by the reinforcement of the north-westerly wind (Figure 34(b,d)). These conditions are responsible for intensified meridional temperature gradients east of the TP and along the Pacific coast which enhance the baroclinicity (see positive anomalies in the Eady growth rate west and east of the chinese coastline Chinese coastline at latitudes 20–40 N, Figure 6(b)). Since Given that the Eady growth rate (definition in) measures the environmental conditions favourable to instability atmospheric baroclinic instability (see definition in Methods), we expect the strengthening of the jet at the entrance of the Pacific basin (Figure 4(c)) to be induced by more synoptic disturbances breaking and depositing zonal momentum in the mean westerly flow. Moreover, cyclogenesis is high to the increased eddy momentum deposition east of the TP and over the East China Sea from, regions where cyclogenesis is climatologically high in mid winter (Priestley et al., 2020; Schemm et al., 2021). In the CMIP6 composite we cannot verify the relation between the transient eddies and the mean flow due to the unavailability of daily frequency data. Nonetheless, the An analysis of the eddy feedback on the zonal flow

is presented in the discussion of the for the idealised “TP+MP experiment” ~~, which generally confirms~~ generally coherent
285 with the results of the CMIP6 composite analysis ~~and~~ supports the hypothesis that the jet ~~is strengthened by enhanced eddy~~
~~momentum deposition. strengthening is induced by an intensification (weakening) of the synoptic activity upstream and to the~~
~~south (north) of the jet maximum. This will be described in more detail in the paragraphs dedicated to the idealised experiments.~~

~~One might wonder why~~ The strong surface heat flux anomalies ~~are~~ present over the Pacific basin in the “cold TP composite”
290 (Figure 3(b,c)) ~~. In the “cold TP composite” the are related to the~~ strengthening of the Pacific jet over and downstream of the
East China Sea (Figure 4(c)) ~~extends, which extend~~ down to the near-surface level (~~not shown~~) ~~and intensifies~~ green arrows in
Figure 3(c)) and intensify the advection of cold air masses over the ocean (Figure 6(a)) ~~, reinforcing the surface sensible heat flux~~
~~(Figure 3(b)) The release of heat thus exerted into the lower layers of the atmosphere restores the . Indeed, cold air temperatures~~
and strong winds in the boundary layer reinforce the surface turbulent heat fluxes by the sea surface. We note that the relation
295 between (i) cold TP temperatures, (ii) strong low-level baroclinicity (Hotta and Nakamura, 2011; Papritz and Spengler, 2015),
~~with a positive feedback on the local generation of synoptic eddies, hence on the strength of the Pacific jet. winds entering the~~
Pacific basin south of Japan and (iii) strong sensible heat fluxes from the ocean surface over the South China Sea, shows a linear
tendency across the CMIP6 models (e.g. the correlation coefficient between (i) and (iii) is -0.85, where (i) is the near-surface
temperature in the TP box (black box in Figure 3(b)) and (iii) is the surface sensible heat flux in a [25-40 N, 120-135 E] box).
300 This confirms that the impact of the TP thermal conditions on the dynamical features of East Asia is not just a peculiarity of the
“cold TP composite”, but rather extends to the whole CMIP6 ensemble. Papritz and Spengler (2015) propose a dominant role
of the surface latent heat flux for maintaining the tilt of the isentropic slopes (i.e. baroclinicity) to the east of the mid-latitude
continents. In this case we observe no significant latent heat flux anomaly over the East China Sea, whereas towards the center
of the Pacific there is a ~~In the composite we also observe a significant~~ decrease in the latent heat flux ~~which suppresses the~~
305 ~~fueling of the jet east of 150~~ east of 135 E (cf. Figure 3(c) and Figure 4(e)) associated with a downstream weakening of the
jet (outside the maps’ boundaries). The origin of the negative latent heat flux ~~is unknown, but anomaly~~ may be related to a
subtropical or tropical Pacific signal emerging from the selection of CMIP6 models (Figures 3(a–c), 4(b–d)).

To ~~support~~ argue for the existence of a causal relation linking the cold Asian orography and the enhancement of the East
~~Asia~~ Asian winter monsoon we run an idealised experiment using the model SPEEDY (a perpetual winter simulation with pre-
310 scribed surface temperatures, for details see Section 2). The response of SPEEDY to “TP+MP” forcing - a surface cooling over
~~central~~ Central Asia orography (Figure 4(e)) resembling the pattern of the “cold TP composite” (Figure 4(a)) - in terms of air
temperature, zonal wind and meridional wind at 850 hPa is shown in panels (f–h) of Figure 4. As in the CMIP6 composite, we
find a cold anomaly to the north-east of the TP, with enhanced north-westerly winds downstream of the ~~topography advecting~~
~~excess~~ mountain barrier advecting cold air onto East Asia and over the Pacific (Figure 7(a)). ~~The striking similarity between~~
315 ~~composite and “TP+MP experiment” (cf. panels (b–d) and (f–h) in Figure 4) proves that also in the “cold TP composite”~~
~~the circulation anomalies in the Asia / Pacific sector are generated by the cold surface temperatures over Asian orography.~~
~~Differences in low-level wind are still detected over the Pacific: in the composite the~~ While in the CMIP6 composite the sig-
nificant strengthening of the jet terminates at about 160 E, ~~while it extends zonally to the whole Pacific basin~~ in the “TP+MP

experiment” (not shown); ~~the the strengthening is zonally coherent over the Pacific basin.~~ The positive meridional wind signal
320 over the North Pacific is also different, with a strong positive ~~signal-anomaly~~ extending from 20 to 70° N in the CMIP6 com-
posite (Figure 4(d)), and a weak positive ~~signal-anomaly~~ limited to the high latitudes in the SPEEDY experiment (Figure 4(h)).
~~Nonetheless, these discrepancies do not undermine the analogy between the two cases, in that they are located far relatively~~
~~from the TP region and~~ These discrepancies might be related to the presence of additional signals emerging from the selec-
tion of CMIP6 models, such as Pacific tropical ~~and subtropical~~-forcing and cold North America land temperatures, ~~or from~~
325 ~~the difference between the MMM and the SPEEDY climatology.~~ Nonetheless, they do not undermine the striking similarity
between the “cold TP composite” and the response of the “TP+MP experiment” (cf. panels (b–d) and (f–h) in Figure 4). As
previously noted for the CMIP6 composite, also the response to “TP+MP” cooling corresponds to an intensification of the East
Asian winter monsoon (cf. Jhun and Lee, 2004) and to a positive interference with the atmospheric response to mountain uplift
(cf. Shi et al., 2015).

330 In the “TP+MP experiment” the increase ~~of eddy momentum deposition in the Pacific jet is evident from the map showing the~~
~~divergence of the~~ in the low-level baroclinicity to north-east of the TP and over the Pacific Ocean at latitudes lower than 40° N
(Figure 6(b)), affects the upper-level synoptic activity. The pattern of meridional eddy momentum flux (MEMF, Figure 7(c);
~~see~~). ~~The increase in low-level baroclinicity to the east of the Chinese coast (~~, which is climatologically negative to the
north of the storm track and positive to its south (see e.g. Hoskins et al., 1983), shifts equatorwards. The zonal convergence of
335 meridional eddy momentum is also displaced to the south, and increases inland to the north-east of the TP (negative purple
contours in Figure 7(b)) ~~favours the development of transient eddies which shift the MEMF convergence equatorwards.~~ Such
environmental conditions are supported by the cold advection from the orography over the East China Sea (Figure 7(ac)), where
it reinforces the jet across the tropospheric column (cf. green contours in Figure 8(b) and shading in Figure 4(c)). In the “cold
TP composite” the positive signal in baroclinicity is stronger and localised closer to the coast (Figure 6). Contrarily, the wind in
340 the northern flank of the jet, experiencing reduced momentum convergence from the synoptic disturbances, weakens. The flux
of eddy total energy (TEF, Figure 8(b)); ~~nevertheless it is consistent with the pattern of jet intensification in Figure 4(c), also~~
~~stronger and more localised than in the “TP+MP experiment”~~, representing the propagation of eddy energy along the storm
track, confirms the increase (decrease) in the synoptic activity in correspondence of the region of jet intensification (slowdown).

345 In the papers by White et al. (2017) and Sha et al. (2015) the winter NH circulation is shown to be more impacted by the
presence of the MP than by the TP ~~due to~~, because of the former’s latitudinal position and of its interaction with the Pacific low-
level jet (Held and Ting, 1990). We briefly consider the role of ~~the former by running the so-called~~ thermal anomalies over the
two regions by showing the results of two experiments. In the “MP experiment” ~~,~~ where the cold anomalies ~~over the Tibetan~~
~~Plateau are removed~~ (from the “TP+MP experiment” north of 38 N are selected (Figure 4(i)). In the “TP experiment” the
350 anomalies south of 38 N), ~~leaving a residual negative temperature signal over the Mongolian Plateau are selected,~~ by applying
the function $\exp\{-1/2 \cdot (5\text{lat})^2\}$ beyond 38 N latitude (Figure 4(i); ~~m~~); the smoothing function, although causing some
superposition of the “MP” and “TP” forcing patterns (panels (i,m) of Figure 4), is necessary to avoid numerical divergences
generated by steep meridional temperature gradients.

The low-level response to “MP” forcing shows cold anomalies limited to high mid latitudes (Figure 4(j)) and cold advection centered over Japan (Figure 7(d)). ~~Since the baroclinicity is also~~ The baroclinicity is enhanced at higher latitudes with respect to the “TP+MP experiment” (cf. panels (b) and (e) of Figure 7); ~~Coherently with the changes in the meridional temperature gradients (baroclinicity), and notwithstanding a weak decline in the upper-level eddy energy over the Pacific Ocean north of 40 N (Figure 8(c)), MP cooling strengthens the Pacific jet~~ on its poleward flank (around its maximum intensity (green contours in Figure 8(c) and shading in Figure 4(k))); ~~coherently with the changes in MEMF convergence (Figure 7(fk))~~. Although the results ~~support the relevance of the MP~~ show that thermal forcing on the MP is relevant for the climate of the Pacific sector, ~~TP surface forcing is necessary~~ the position of the forcing is not appropriate to have consistency with the “response of the “TP+MP experiment”, hence with the anomalies emerging in the “cold TP composite”. ~~The latter is in fact fundamental to obtain a strengthening of the baroclinic conditions over East Asia and~~

On the other hand, the “TP experiment” shows strong similarity with the “MP+TP experiment”. It features strong advection of cold temperatures to the south of Japan (Figure 7(g) and 4(n)) which produces baroclinic conditions south of 40 N (Figure 7(h)). In correspondence of the low-level Eady growth rate increase, the upper-troposphere synoptic activity is intensified (see TEF in Figure 8(d)) and is associated, as in “TP+MP”, with a southward shift and upstream intensification of the meridional eddy momentum convergence (purple contours in Figure 7(i)). This explains the strengthening and equatorward shift of the Pacific jet ~~to the east of the Chinese coast, i.e. for the overall intensification the East Asia winter monsoon.~~ (green contours in Figure 8(d) and shading in Figure 4(o)). Hence, although the response to “TP” cooling is weaker in intensity compared to “TP+MP” cooling, surface forcing over the TP region is fundamental to obtain the environmental conditions that produce the atmospheric patterns in the latter experiment. The inclusion of MP cooling then reinforces the circulation anomalies in the western Pacific (see e.g. TEF and zonal-wind anomalies in Figure 8(b–d)).

4 Conclusions

By comparing a selection of CMIP6 historical simulations - the “cold Tibetan Plateau (TP) composite” - with an idealised AGCM simulation, we show how cold temperatures over Central Asia orography influence the winter atmospheric circulation over East Asia and the North Pacific. Colder than average Asian high plateaux strengthen the tropospheric heat sink and ~~intensify the East Asia~~ the East Asian winter monsoon, ~~leading to stronger~~ corresponding to an intensification of the north-westerly winds and ~~cold advection downstream of the orographic features of the downstream advection of cold temperature.~~ Over the East China Sea, the enhancement of the advection of cold northerly air from the continent and of the surface heat flux from the ocean contribute to the intensification of the low-level baroclinicity. The ~~idealised experiment shows results of the idealised experiment show~~ that low-level baroclinic conditions over the East China Sea favour the development of transient atmospheric perturbations which deposit additional eddy momentum on the mean zonal flow, reinforcing the ~~equatorward flank jet stream mainly upstream~~ of the Pacific jet basin and on its equatorward flank (Hoskins et al., 1983; Hoskins and Valdes, 1990).

We note that the cooling of Central Asia orography interestingly corresponds to an overall amplification of the response to the uplift of the orography itself, presented in the works by Shi et al. (2015); Sha et al. (2015); White et al. (2017). This is in line with the results of the highly idealised study by Ringler and Cook (1999), which shows how the atmospheric response to simple patterns of orographic forcing is amplified (nonlinearly) by superposed cooling.

390 Building on previous literature that investigates the relative role of the Tibetan and Mongolian Plateaux on the downstream winter climate by removing or adding regional orography (Shi et al., 2015; Sha et al., 2015; White et al., 2017), we apply a similar approach to surface temperature forcing. ~~A~~ In a second set of idealised simulations is presented where, cold anomalies are confined to the ~~region with Mongolian orography~~ regions of the Mongolian or of the Tibetan Plateau. The response ~~still consists in a strengthening of the zonal winds over the Pacific, however shifted northward with respect to the experiment with~~ extended surface cooling, ~~due to weakened advection of cold air to the east of the Tibetan Plateau.~~ We conclude to Tibetan Plateau cooling only, shows strong resemblance with the response to the total cooling pattern, supporting the fact that the TP region is fundamental for setting ~~the ideal conditions~~ atmospheric conditions ideal for the intensification of the East ~~Asia winter monsoon, as detected~~ Asian winter monsoon and of the Pacific jet, as in the CMIP6 models contributing to the “cold TP composite”. ~~Still, changes in the Mongolian Plateau land temperature are relevant to understand future projections of the winter~~ season ~~The response to Mongolian Plateau cooling still consists in a strengthening of the zonal winds over the Pacific sector~~ (Xu et al., 2016), and reinforces the atmospheric response to Tibetan Plateau cooling. However, due to ~~weakened advection of cold air to the east of the Tibetan Plateau, the jet intensification is shifted northward with respect to experiments with TP or total surface cooling.~~ We note that a limited superposition of the two regional forcing patterns is present, due to a latitudinal smoothing of the anomalies in the TP forcing experiment.

405 ~~CMIP6 climate~~ The influence of East Asian surface temperature anomalies on the climate downstream is particularly relevant in the context of climate modelling, since state-of-the-art models are often affected by a cold surface and near-surface temperature bias ~~in~~ over East Asia (Wei et al., 2014; Gong et al., 2014), which is accentuated over the Tibetan Plateau region ~~(Peng et al., 2022; Fan et al., 2020) and show limited improvements despite the massive~~ (Peng et al., 2022; Fan et al., 2020, Figure 1.) Limited improvements have been detected, despite the model developments of the recent years (e.g. across CMIP phases, Bock et al., 2020; Lun et al., 2021; Hu et al., 2022). ~~Chen et al. (2017)~~ The issue is analysed in considerable detail by Chen et al. (2017), who decompose the surface energy budget over the TP and show that the processes causing ~~cold biases~~ involve anomalous snow cover with a cascade of consequences on surface albedo surface and low-level cold biases are physically interlinked, and involve snow cover (and surface albedo), low-level water vapor content ~~and downward longwave radiation,~~ which, downward longwave and shortwave radiation. The anomalies in the low-level heat fluxes ultimately result in a cooling of the surface. ~~This boundary layer.~~

The results of this work suggests that ~~deviations from the observed land temperature~~ thermal conditions over high Central Asia plateaux foster significant changes in the large-scale circulation ~~biases~~ on the lee side of the orography. Specifically, Relating this to the cold Tibetan Plateau temperature bias measured across many climate models, it is possible to assert that such a surface anomaly potentially produces atmospheric biases over East Asia and the western North Pacific. Specifically, models characterised by colder-than-average temperatures over Central Asian plateaux present a strengthening of the East ~~Asia~~

Asian winter monsoon, affecting the atmospheric conditions of the highly inhabited eastern coast of China and the Pacific jet, is found in models characterised by colder-than-average temperatures over Central Asia plateaux. Although not considered in this work, the results also provide a new perspective on elevation dependent warming (EDW), implying that a stronger warming of Asian orography with respect to other land regions may be important not only for the local climate, but also for the mean atmospheric conditions downstream. Further work is needed to assess such an impact of EDW.

425 ~~Based on these findings,~~ Finally, based on the findings here presented, we prospect that advances in the representation of surface processes over complex orography are expected to reduce temperature and circulation biases and to will improve the modelling of the mean climate downstream of the ~~Central Asia plateaux.~~ Stronger Asian high plateaux and the inter-model coherence would also reinforce the confidence in climate projections for the next decades. Similarly, approaches such as the

430 ~~“emerging constraints” (Hall et al., 2019) applied to the feedback between surface temperatures over orography and the local energy budget, may be useful to reduce the uncertainty of the above-mentioned~~ spread in this region, with possible impacts on the confidence of regional multi-model climate projections. On a different time scale, works analysing subseasonal-to-seasonal forecasts over East Asia find a significant influence by surface anomalies over the Tibetan Plateau (e.g. Li et al., 2018; Xue et al., 2021), implying that shorter-term operational forecasting could also benefit from advances in the modelling of land–

435 ~~atmosphere interaction over Central Asia plateaux. Otherwise, within the state of the art of model ensembles (e.g. CMIP6), the “emergent constraints” approach (Hall et al., 2019), applied to the feedback between surface temperatures over orography and the local energy budget, can become a useful means of reducing present uncertainty in East Asian climate projections.~~

Data availability. The CMIP6 dataset is publicly available at <https://esgf-node.llnl.gov/projects/cmip6/>. Download information on the AGCM “SPEEDY” can be found at the link <https://www.ictp.it/research/esp/models/speedy.aspx>.

440 *Author contributions.* All authors conceived the study and contributed to the interpretation and discussion of the results. A. P. performed the analyses and wrote the paper.

Competing interests. No competing interests are present.

Acknowledgements. A. P. is thankful to Gwendal Rivière for insightful discussion and advice. The authors also thank three anonymous reviewers, whose comments and suggestions contributed in improving the quality of the paper.

445 **References**

- Bock, L., Lauer, A., Schlund, M., Barreiro, M., Bellouin, N., Jones, C., Meehl, G., Predoi, V., Roberts, M., and Eyring, V.: Quantifying progress across different CMIP phases with the ESMValTool, *Journal of Geophysical Research: Atmospheres*, 125, e2019JD032 321, 2020.
- Bolin, B.: On the influence of the earth's orography on the general character of the westerlies, *Tellus*, 2, 184–195, 1950.
- 450 Broccoli, A. J. and Manabe, S.: The effects of orography on midlatitude Northern Hemisphere dry climates, *Journal of Climate*, 5, 1181–1201, 1992.
- Chan, J. C. and Li, C.: The east Asia winter monsoon, in: *East Asian Monsoon*, pp. 54–106, World Scientific, 2004.
- Charney, J. G. and Eliassen, A.: A numerical method for predicting the perturbations of the middle latitude westerlies, *Tellus*, 1, 38–54, 1949.
- Chen, X., Liu, Y., and Wu, G.: Understanding the surface temperature cold bias in CMIP5 AGCMs over the Tibetan Plateau, *Advances in*
455 *Atmospheric Sciences*, 34, 1447–1460, 2017.
- Chen, Z., Wu, R., and Wang, Z.: Impact of Autumn-Winter Tibetan Plateau Snow Cover Anomalies on the East Asian Winter Monsoon and Its Interdecadal Change, *Frontiers in Earth Science*, 9, 569, 2021.
- Clark, M. P. and Serreze, M. C.: Effects of variations in East Asian snow cover on modulating atmospheric circulation over the North Pacific Ocean, *Journal of Climate*, 13, 3700–3710, 2000.
- 460 Cohen, J., Saito, K., and Entekhabi, D.: The role of the Siberian high in Northern Hemisphere climate variability, *Geophysical Research Letters*, 28, 299–302, 2001.
- Cohen, J., Furtado, J. C., Jones, J., Barlow, M., Whittleston, D., and Entekhabi, D.: Linking Siberian snow cover to precursors of stratospheric variability, *Journal of Climate*, 27, 5422–5432, 2014.
- Drouard, M., Rivière, G., and Arbogast, P.: The link between the North Pacific climate variability and the North Atlantic Oscillation via
465 downstream propagation of synoptic waves, *Journal of Climate*, 28, 3957–3976, 2015.
- Duan, A. and Wu, G.: Weakening trend in the atmospheric heat source over the Tibetan Plateau during recent decades. Part I: Observations, *Journal of Climate*, 21, 3149–3164, 2008.
- Fan, X., Miao, C., Duan, Q., Shen, C., and Wu, Y.: The performance of CMIP6 versus CMIP5 in simulating temperature extremes over the global land surface, *Journal of Geophysical Research: Atmospheres*, 125, e2020JD033 031, 2020.
- 470 Garfinkel, C. I., Hartmann, D. L., and Sassi, F.: Tropospheric precursors of anomalous Northern Hemisphere stratospheric polar vortices, *Journal of Climate*, 23, 3282–3299, 2010.
- Gong, H., Wang, L., Chen, W., Wu, R., Wei, K., and Cui, X.: The climatology and interannual variability of the East Asian winter monsoon in CMIP5 models, *Journal of Climate*, 27, 1659–1678, 2014.
- Hahn, D. G. and Manabe, S.: The role of mountains in the south Asian monsoon circulation, *Journal of the Atmospheric Sciences*, 32,
475 1515–1541, 1975.
- Hall, A., Cox, P., Huntingford, C., and Klein, S.: Progressing emergent constraints on future climate change, *Nature Climate Change*, 9, 269–278, 2019.
- Held, I. M. and Ting, M.: Orographic versus thermal forcing of stationary waves: The importance of the mean low-level wind, *Journal of Atmospheric Sciences*, 47, 495–500, 1990.
- 480 Henderson, G. R., Leathers, D. J., and Hanson, B.: Circulation response to Eurasian versus North American anomalous snow scenarios in the Northern Hemisphere with an AGCM coupled to a slab ocean model, *Journal of climate*, 26, 1502–1515, 2013.

- Henderson, G. R., Peings, Y., Furtado, J. C., and Kushner, P. J.: Snow–atmosphere coupling in the Northern Hemisphere, *Nature Climate Change*, 8, 954–963, 2018.
- Hoskins, B. J. and Karoly, D. J.: The steady linear response of a spherical atmosphere to thermal and orographic forcing, *Journal of Atmospheric Sciences*, 38, 1179–1196, 1981.
- Hoskins, B. J. and Valdes, P. J.: On the existence of storm-tracks, *Journal of Atmospheric Sciences*, 47, 1854–1864, 1990.
- Hoskins, B. J., James, I. N., and White, G. H.: The shape, propagation and mean-flow interaction of large-scale weather systems, *Journal of Atmospheric Sciences*, 40, 1595–1612, 1983.
- Hotta, D. and Nakamura, H.: On the significance of the sensible heat supply from the ocean in the maintenance of the mean baroclinicity along storm tracks, *Journal of Climate*, 24, 3377–3401, 2011.
- Hu, Q., Hua, W., Yang, K., Ming, J., Ma, P., Zhao, Y., and Fan, G.: An assessment of temperature simulations by CMIP6 climate models over the Tibetan Plateau and differences with CMIP5 climate models, *Theoretical and Applied Climatology*, 148, 223–236, 2022.
- Jhun, J.-G. and Lee, E.-J.: A new East Asian winter monsoon index and associated characteristics of the winter monsoon, *Journal of Climate*, 17, 711–726, 2004.
- Kucharski, F., Molteni, F., and Bracco, A.: Decadal interactions between the western tropical Pacific and the North Atlantic Oscillation, *Climate dynamics*, 26, 79–91, 2006.
- Kucharski, F., Molteni, F., King, M. P., Farneti, R., Kang, I.-S., and Feudale, L.: On the need of intermediate complexity general circulation models: A “SPEEDY” example, *Bulletin of the American Meteorological Society*, 94, 25–30, 2013.
- Li, J., Miao, C., Wei, W., Zhang, G., Hua, L., Chen, Y., and Wang, X.: Evaluation of CMIP6 global climate models for simulating land surface energy and water fluxes during 1979–2014, *Journal of Advances in Modeling Earth Systems*, 13, e2021MS002515, 2021.
- Li, W., Guo, W., Qiu, B., Xue, Y., Hsu, P.-C., and Wei, J.: Influence of Tibetan Plateau snow cover on East Asian atmospheric circulation at medium-range time scales, *Nature communications*, 9, 1–9, 2018.
- Liu, A., Huang, Y., and Huang, D.: Inter-model Spread of the Simulated Winter Surface Air Temperature over the Eurasian Continent and the Physical Linkage to the Jet Streams from the CMIP6 Models, *Journal of Geophysical Research: Atmospheres*, p. e2022JD037172, 2022.
- Liu, L., Zhang, W., Lu, Q., and Wang, G.: Variations in the Sensible Heating of Tibetan Plateau and Related Effects on Atmospheric Circulation Over South Asia, *Asia-Pacific Journal of Atmospheric Sciences*, 57, 499–510, 2021.
- Lun, Y., Liu, L., Cheng, L., Li, X., Li, H., and Xu, Z.: Assessment of GCMs simulation performance for precipitation and temperature from CMIP5 to CMIP6 over the Tibetan Plateau, *International Journal of Climatology*, 41, 3994–4018, 2021.
- Manabe, S. and Terpstra, T. B.: The effects of mountains on the general circulation of the atmosphere as identified by numerical experiments, *Journal of Atmospheric Sciences*, 31, 3–42, 1974.
- Molteni, F.: Atmospheric simulations using a GCM with simplified physical parametrizations. I: Model climatology and variability in multi-decadal experiments, *Climate Dynamics*, 20, 175–191, 2003.
- Papritz, L. and Spengler, T.: Analysis of the slope of isentropic surfaces and its tendencies over the North Atlantic, *Quarterly Journal of the Royal Meteorological Society*, 141, 3226–3238, 2015.
- Peng, Y., Duan, A., Hu, W., Tang, B., Li, X., and Yang, X.: Observational constraint on the future projection of temperature in winter over the Tibetan Plateau in CMIP6 models, *Environmental Research Letters*, 2022.
- Portal, A., Pasquero, C., D’Andrea, F., Davini, P., Hamouda, M. E., and Rivière, G.: Influence of Reduced Winter Land–Sea Contrast on the Midlatitude Atmospheric Circulation, *Journal of Climate*, 35, 2637–2651, 2022.

- Priestley, M. D., Ackerley, D., Catto, J. L., Hodges, K. I., McDonald, R. E., and Lee, R. W.: An overview of the extratropical storm tracks in
520 CMIP6 historical simulations, *Journal of Climate*, 33, 6315–6343, 2020.
- Priestley, M. D., Ackerley, D., Catto, J. L., and Hodges, K. I.: Drivers of biases in the CMIP6 extratropical storm tracks. Part 1: Northern
Hemisphere, *Journal of Climate*, pp. 1–37, 2022.
- Rayner, N., Parker, D. E., Horton, E., Folland, C. K., Alexander, L. V., Rowell, D., Kent, E. C., and Kaplan, A.: Global analyses of sea surface
temperature, sea ice, and night marine air temperature since the late nineteenth century, *Journal of Geophysical Research: Atmospheres*,
525 108, 2003.
- Ringler, T. D. and Cook, K. H.: Understanding the seasonality of orographically forced stationary waves: Interaction between mechanical
and thermal forcing, *Journal of the atmospheric sciences*, 56, 1154–1174, 1999.
- Sato, T.: Influences of subtropical jet and Tibetan Plateau on precipitation pattern in Asia: Insights from regional climate modeling, *Quater-
nary International*, 194, 148–158, 2009.
- 530 Schemm, S., Wernli, H., and Binder, H.: The storm-track suppression over the western North Pacific from a cyclone life-cycle perspective,
Weather and Climate Dynamics, 2, 55–69, 2021.
- Sha, Y., Shi, Z., Liu, X., and An, Z.: Distinct impacts of the Mongolian and Tibetan Plateaus on the evolution of the East Asian monsoon,
Journal of Geophysical Research: Atmospheres, 120, 4764–4782, 2015.
- Shi, Z., Liu, X., Liu, Y., Sha, Y., and Xu, T.: Impact of Mongolian Plateau versus Tibetan Plateau on the westerly jet over North Pacific
535 Ocean, *Climate Dynamics*, 44, 3067–3076, 2015.
- Smagorinsky, J.: The dynamical influence of large-scale heat sources and sinks on the quasi-stationary mean motions of the atmosphere,
Quarterly Journal of the Royal Meteorological Society, 79, 342–366, 1953.
- Su, F., Duan, X., Chen, D., Hao, Z., and Cuo, L.: Evaluation of the global climate models in the CMIP5 over the Tibetan Plateau, *Journal of
climate*, 26, 3187–3208, 2013.
- 540 Ting, M.: The stationary wave response to a midlatitude SST anomaly in an idealized GCM, *Journal of the atmospheric sciences*, 48, 1249–
1275, 1991.
- Trenberth, K. E.: Interactions between orographically and thermally forced planetary waves, *Journal of Atmospheric Sciences*, 40, 1126–
1153, 1983.
- Wei, K., Xu, T., Du, Z., Gong, H., and Xie, B.: How well do the current state-of-the-art CMIP5 models characterise the climatology of the
545 East Asian winter monsoon?, *Climate dynamics*, 43, 1241–1255, 2014.
- White, R., Battisti, D., and Roe, G.: Mongolian mountains matter most: Impacts of the latitude and height of Asian orography on Pacific
wintertime atmospheric circulation, *Journal of Climate*, 30, 4065–4082, 2017.
- Wilks, D. S.: *Statistical methods in the atmospheric sciences*, vol. 100, Academic press, 2011.
- Wu, G., Duan, A., Liu, Y., Mao, J., Ren, R., Bao, Q., He, B., Liu, B., and Hu, W.: Tibetan Plateau climate dynamics: recent research progress
550 and outlook, *National Science Review*, 2, 100–116, 2015.
- Xu, M., Xu, H., and Ma, J.: Responses of the East Asian winter monsoon to global warming in CMIP5 models, *International Journal of
Climatology*, 36, 2139–2155, 2016.
- Xue, Y., Yao, T., Boone, A. A., Diallo, I., Liu, Y., Zeng, X., Lau, W. K., Sugimoto, S., Tang, Q., Pan, X., et al.: Impact of initialized land
surface temperature and snowpack on subseasonal to seasonal prediction project, phase i (Is4p-i): organization and experimental design,
555 *Geoscientific Model Development*, 14, 4465–4494, 2021.

- Xue, Y., Diallo, I., Boone, A. A., Yao, T., Zhang, Y., Zeng, X., David Neelin, J., Lau, W. K., Pan, Y., Liu, Y., et al.: Spring Land Temperature in Tibetan Plateau and Global-Scale Summer Precipitation–Initialization and Improved Prediction, *Bulletin of the American Meteorological Society*, 2022.
- Yanai, M. and Wu, G.-X.: Effects of the Tibetan plateau, in: *The Asian Monsoon*, pp. 513–549, Springer, 2006.
- 560 Yanai, M., Li, C., and Song, Z.: Seasonal heating of the Tibetan Plateau and its effects on the evolution of the Asian summer monsoon, *Journal of the Meteorological Society of Japan. Ser. II*, 70, 319–351, 1992.
- Ye, D.-Z. and Wu, G.-X.: The role of the heat source of the Tibetan Plateau in the general circulation, *Meteorology and Atmospheric Physics*, 67, 181–198, 1998.
- Yeh, T., Wetherald, R., and Manabe, S.: A model study of the short-term climatic and hydrologic effects of sudden snow-cover removal, 565 *Monthly Weather Review*, 111, 1013–1024, 1983.
- Yihui, D. and Chan, J. C.: The East Asian summer monsoon: an overview, *Meteorology and Atmospheric Physics*, 89, 117–142, 2005.
- Zhang, Y., Sperber, K. R., and Boyle, J. S.: Climatology and interannual variation of the East Asian winter monsoon: Results from the 1979–95 NCEP/NCAR reanalysis, *Monthly weather review*, 125, 2605–2619, 1997.

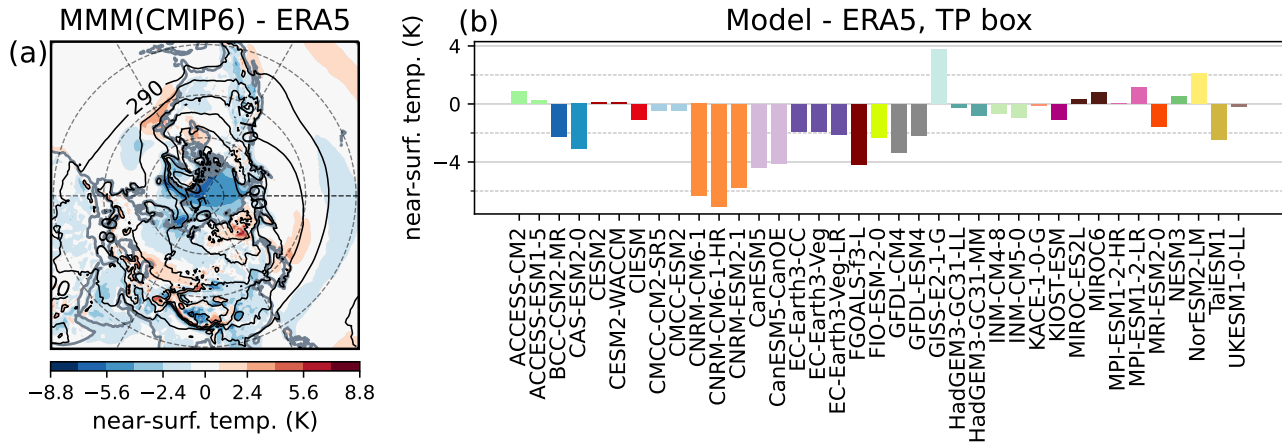


Figure 1. (a) The multi-model mean bias with respect to ERA5 in the Jan-Feb near-surface temperature spread in CMIP6 historical climatology 1979–2008 for Jan-Feb, with the MMM field-ERA5 climatology in contours, and (b) the MMM orographic elevation. The individual model biases over the TP box [25-40 N, 70-105 E] (see black box in panel (b) is used to compute the Tibetan Plateau index for near-surface temperature; the “cold TP composite” presented in Figures of Figure 3–6 is based on such index. The dotted boxes in panel (b) indicate the mountainous regions here named Tibetan Plateau or TP (green) and Mongolian Plateau or MP (orange))

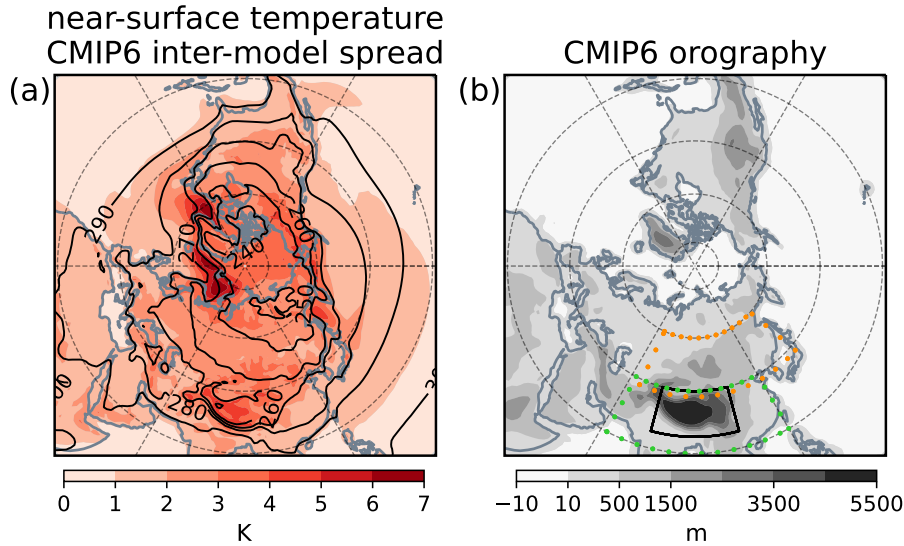


Figure 2. (a) The inter-model spread (standard deviation) in the Jan-Feb near-surface temperature climatology for CMIP6 historical 1979–2008 simulations, with the MMM field in contours, and (b) the MMM orographic elevation. The black longitude-latitude contour in panel (b), of range [25–40 N, 70–105 E], is the TP box used to compute the Tibetan Plateau index for near-surface temperature; the model biases in Figure 1(b) and the “cold TP composite” presented in Figures 3–6 are based on such index. The dotted boxes in panel (b) indicate the mountainous regions here named Tibetan Plateau or TP region (green) and Mongolian Plateau or MP region (orange)

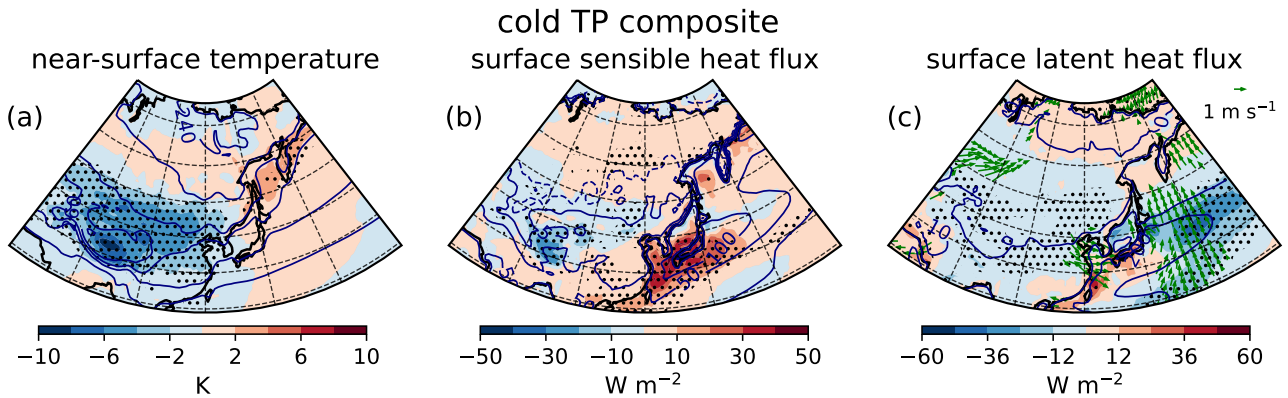


Figure 3. From the “cold TP composite” the anomalies of (a) near-surface temperature, (b) sensible and (c) latent surface heat flux (stippling above the 95% significance level upward) and 1000 hPa horizontal wind vector (green arrows). Stippling and arrows indicate where anomalies exceed the 95th percentile in a randomly extracted 6-model composite distribution, see Methods. The respective MMM climatologies are displayed in contours ($cl=[\pm 5,+25,+50,+100,+200]$ $W m^{-2}$ for sensible heat flux, $cl=[0,+300,10,+100,+200,+400]$ $KW m^{-2}$ for the latent heat fluxes flux)

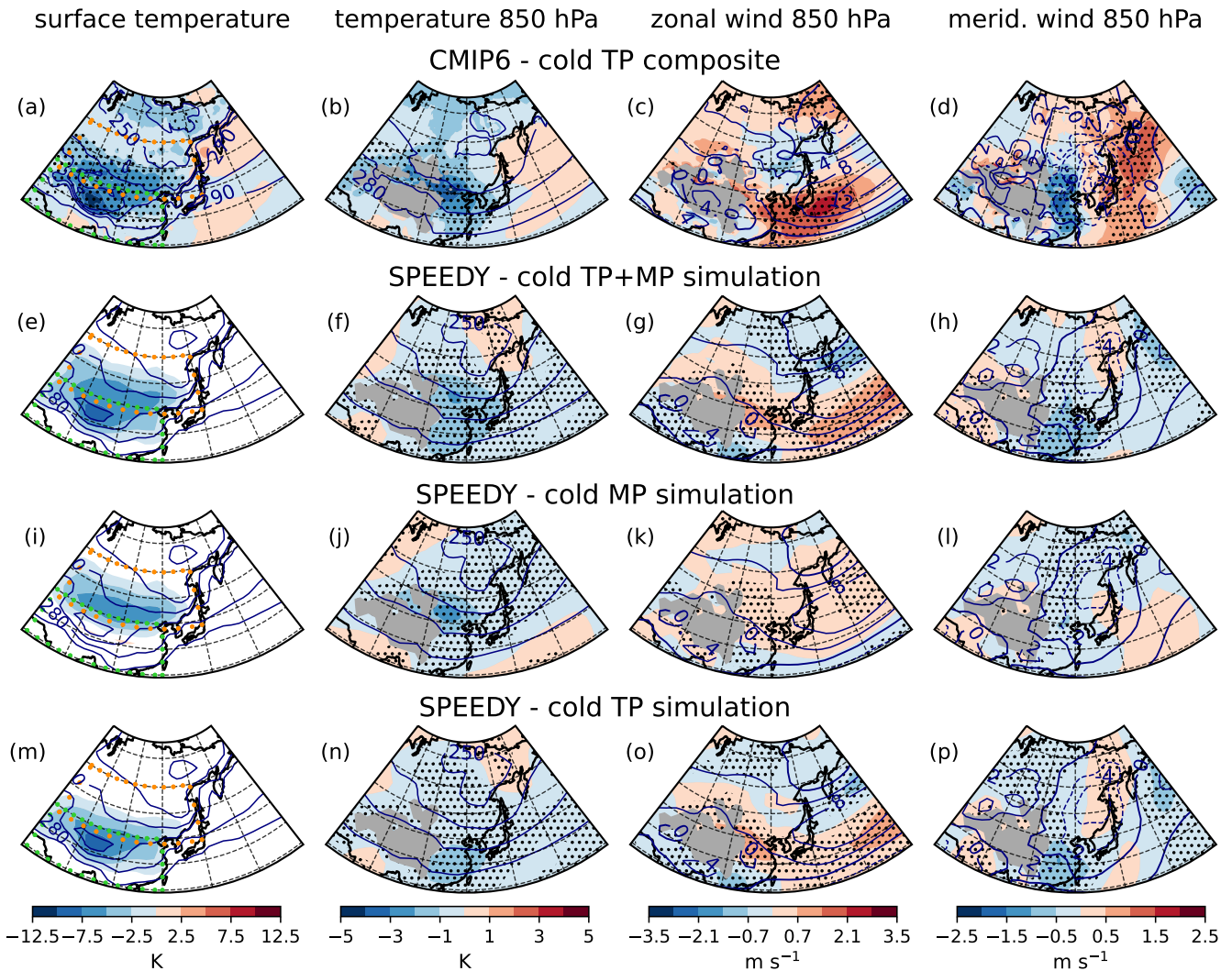


Figure 4. The “cold TP composite” anomalies of (a) surface temperature and 850-hPa (b) air temperature, (c) zonal wind, (d) meridional wind. The respective MMM climatologies are displayed in contours. The response of the model SPEEDY to “TP+MP” and, “MP” and “TP” surface-temperature forcing (panels (e,i,m)) in terms of 850-hPa (f,j,n) temperature, (g,k,o) zonal wind, (h,l,p) meridional wind; the control run is shown in contours. Stippling indicates that shows the anomalies exceeding the 95% significance level (95th percentile of a randomly extracted distribution (see Methods)). Green and orange dotted boxes in panels (a,e,i,m) indicate the mountainous regions/areas named TP region and MP region, respectively. Grey shading masks orography exceeding 1400 m

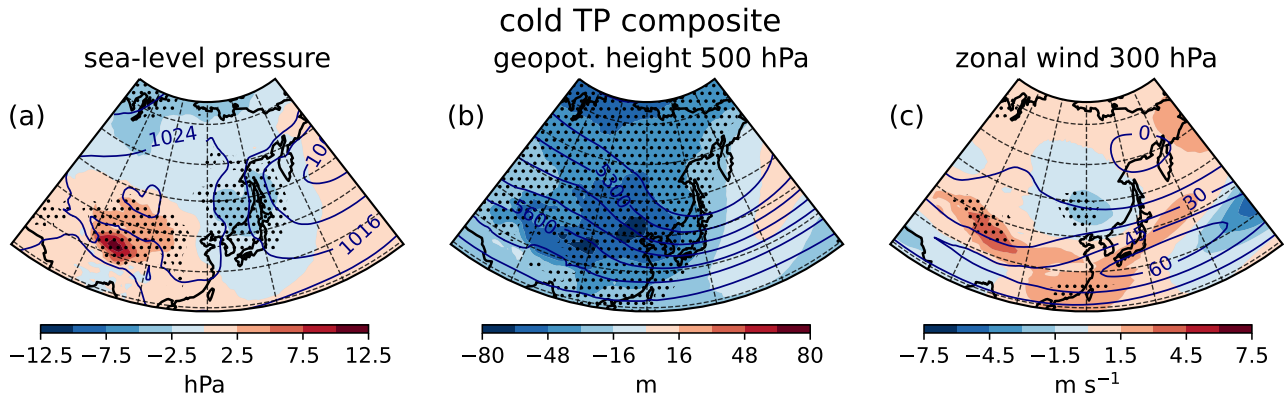


Figure 5. The “cold TP composite” anomalies of (a) sea-level pressure, (b) 500 hPa geopotential height and (c) 300 hPa zonal wind; the respective MMM climatologies in contours. Stippling shows the anomalies exceeding the 95th percentile in a randomly extracted 6-model composite distribution, see Methods

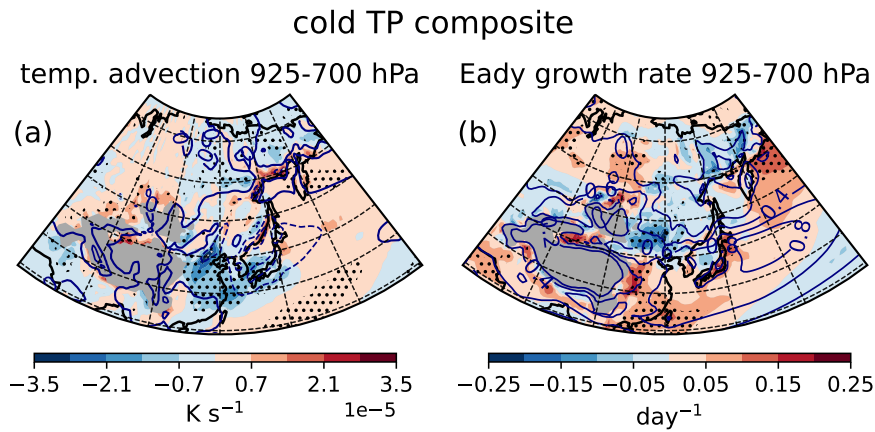


Figure 6. The “cold TP composite” anomalies of (a) temperature advection by the mean flow ($\mathbf{u} \cdot \nabla T$) averaged over the pressure-levels 925 to 700 hPa, (b) Eady growth rate between 925 and 700 hPa, and the respective MMM climatologies in contours (contour interval = $4 \times 10^{-5} \text{ K s}^{-1}$ for temperature advection, stippling above for anomalies exceeding the 95% significance level, 95th percentile in a randomly extracted 6-model composite distribution, see Methods). Grey shading masks orography exceeding 1400 m

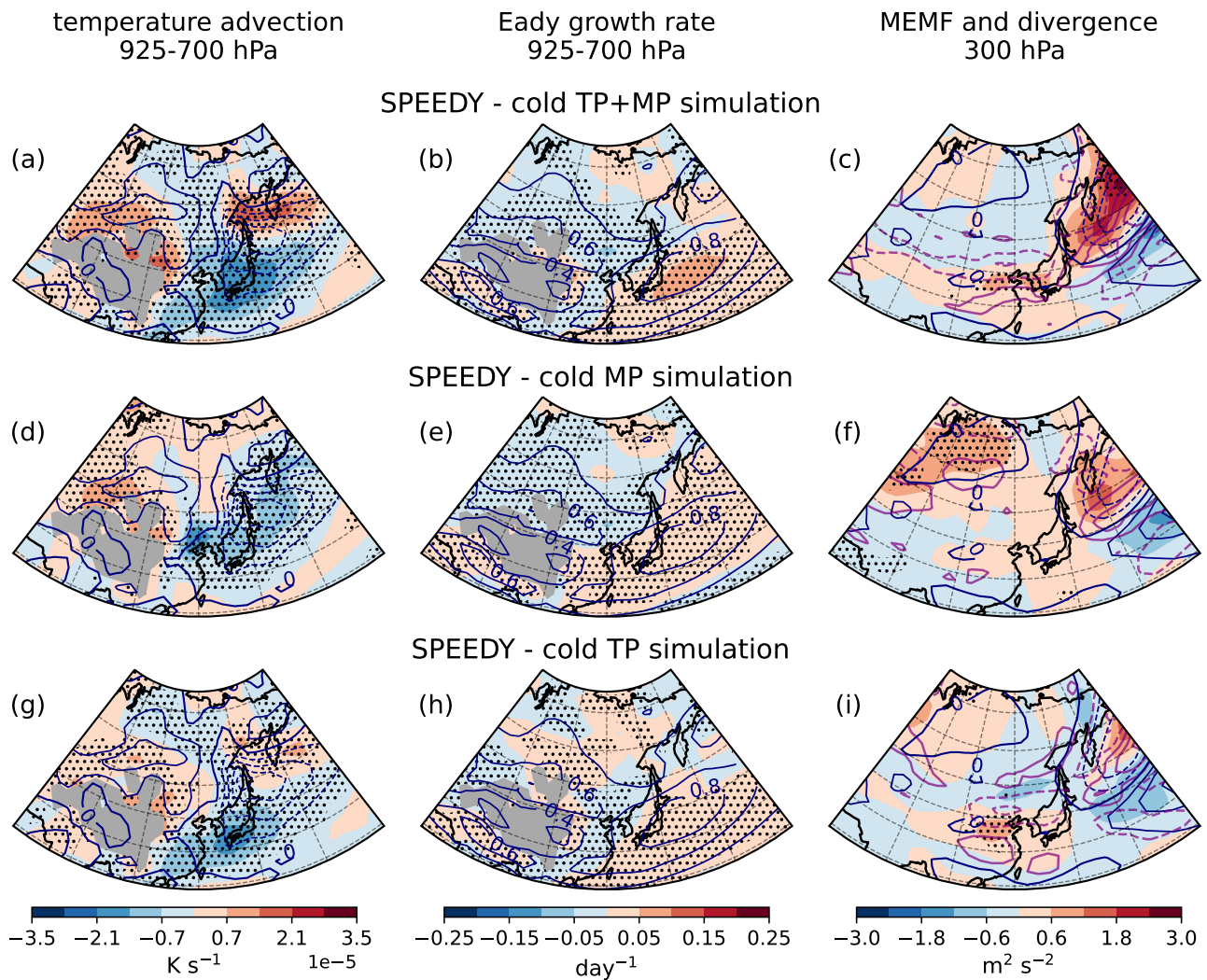


Figure 7. The response of the model SPEEDY to “TP+MP” and “MP” and “TP” surface-temperature forcing in terms of (a,d,g) temperature advection by the mean flow ($u \cdot \nabla T$) averaged over the pressure levels 925 to 700 hPa, (b,e,h) Eady growth rate between 925 and 700 hPa, (c,f,i) divergence of the meridional eddy momentum flux (MEMF) at 850-300 hPa and its divergence (in purple contours for $cl=[\pm 5, \pm 15, +25]e-7 \text{ ms}^{-2}$). The control run is shown in contours ($ci=4e-5 \text{ K s}^{-1}$ for temperature advection, $ci=3e-65 \text{ m}^2 \text{ s}^{-2}$ for MEMF divergence) and stippling indicates where the anomalies exceed the 95th percentile of a randomly extracted distribution (see Methods). Grey shading masks orography exceeding 1400 m

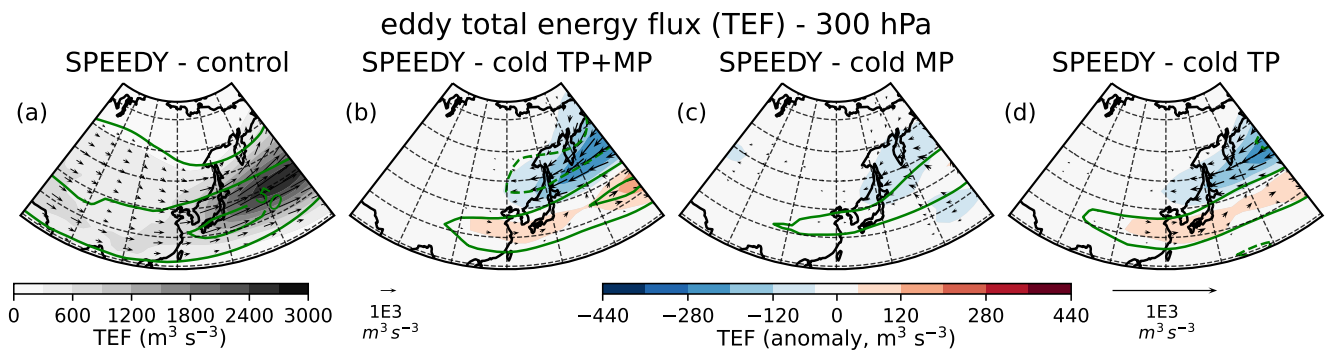


Figure 8. (a) The 300 hPa eddy total energy flux (TEF) climatology in the SPEEDY control integration, and the TEF response to (b) “TP+MP”, (c) “MP” and (d) “TP” surface-temperature forcing. The zonal wind is shown in green contours ($c_i=20 \text{ m s}^{-1}$ for the control climatology in panel (a), $c_i=[\pm 1, \pm 3] \text{ m s}^{-1}$ for the response in panels (b-d))

Table 1. List of CMIP6 climate models

Model Name	Member Id.	Institution	Horizontal Resolution (lon × lat)
ACCESS-CM2	1	Australian Research Council Centre of Excellence for Climate System Science & Commonwealth Scientific and Industrial Research Organisation (AUS)	$1.9^\circ \times 1.3^\circ$
ACCESS-ESM1-5	1	Commonwealth Scientific and Industrial Research Organisation (AUS)	$1.9^\circ \times 1.2^\circ$
BCC-CSM2-MR	1	Beijing Climate Center (CHN)	$1.1^\circ \times 1.1^\circ$
<u>CanESM5</u>	<u>1</u>	<u>Canadian Centre for Climate Modelling and Analysis (CAN)</u>	$2.8^\circ \times 2.8^\circ$
<u>CanESM5-CanOE</u>	<u>1</u>	<u>as above</u>	$1.9^\circ \times 1.9^\circ$
CAS-ESM2-0	2	Chinese Academy of Sciences (CHN)	$1.4^\circ \times 1.4^\circ$
CESM2	2	National Center for Atmospheric Research, Climate and Global Dynamics Laboratory (USA)	$1.3^\circ \times 0.9^\circ$
CESM2-WACCM	1	as above	$1.3^\circ \times 0.9^\circ$
CIESM	1	Department of Earth System Science, Tsinghua University (CHN)	$0.9^\circ \times 1.3^\circ$
CMCC-CM2-SR5	1	Fondazione Centro Euro-Mediterraneo sui Cambiamenti Climatici (ITA)	$0.9^\circ \times 1.3^\circ$
CMCC-ESM2	1	as above	$0.9^\circ \times 1.3^\circ$
CNRM-CM6-1	1	Centre National de Recherches Meteorologiques & Centre Européen de Recherche et de Formation Avancée en Calcul Scientifique (FRA)	$1.4^\circ \times 1.4^\circ$
CNRM-CM6-1-HR	1	as above	$0.5^\circ \times 0.5^\circ$
CNRM-ESM2-1	1	as above CanESM5	+ Canadian Cent
CanESM5-CanOE + as above	1	EC-Earth consortium (visit https://ec-earth.org/consortium/)	$0.7^\circ \times 0.7^\circ$
EC-Earth3-CC	1	as above	$0.7^\circ \times 0.7^\circ$
EC-Earth3-Veg	1	as above	$1.1^\circ \times 1.1^\circ$
EC-Earth3-Veg-LR	1	as above	$1.3^\circ \times 1^\circ$
FGOALS-f3-L	1	Chinese Academy of Sciences (CHN)	$1.3^\circ \times 1^\circ$
FIO-ESM-2-0	1	Qingdao National Laboratory for Marine Science and Technology & First Institute of Oceanography (CHN)	$1.3^\circ \times 0.9^\circ$
GFDL-CM4	1	National Oceanic and Atmospheric Administration, Geophysical Fluid Dynamics Laboratory (USA)	$1.3^\circ \times 1^\circ$
GFDL-ESM4	1	as above	$1.3^\circ \times 1^\circ$
GISS-E2-1-G	1	Goddard Institute for Space Studies (USA)	$2.5^\circ \times 2^\circ$
HadGEM3-GC31-LL	1	Met Office Hadley Centre (GBR)	$1.9^\circ \times 1.2^\circ$
HadGEM3-GC31-MM	1	as above	$0.8^\circ \times 0.6^\circ$
INM-CM4-8	1	Institute for Numerical Mathematics (RUS)	$2^\circ \times 1.5^\circ$
INM-CM5-0	1	as above	$2^\circ \times 1.5^\circ$
KACE-1-0-G	1	National Institute of Meteorological Sciences/Korea Meteorological Administration (KOR)	$1.3^\circ \times 0.9^\circ$
KIOST-ESM	1	Korea Institute of Ocean Science & Technology (KOR)	$1.9^\circ \times 1.9^\circ$
<u>MIROC6</u>	<u>1</u>	<u>as above</u>	<u>$1.4^\circ \times 1.4^\circ$</u>
MIROC-ES2L	1	Japan Agency for Marine-Earth Science and Technology & Atmosphere and Ocean Research Institute & National Institute for Environmental Studies & RIKEN Center for Computational Science (JPN)	MIROC6- + as above 2.8°
MPI-ESM1-2-HR	1	Max Planck Institute for Meteorology (DEU)	$0.9^\circ \times 0.9^\circ$
MPI-ESM1-2-LR	1	as above	$1.9^\circ \times 1.9^\circ$
MRI-ESM2-0	1	Meteorological Research Institute (JPN)	$1.1^\circ \times 1.1^\circ$
NESM3	1	Nanjing University of Information Science and Technology (CHN)	$1.9^\circ \times 1.9^\circ$
NorESM2-LM	1	NorESM Climate modeling Consortium (visit https://www.noresm.org/consortium/)	$2.5^\circ \times 1.9^\circ$
TaiESM1	1	Research Center for Environmental Changes (TWN)	$0.9^\circ \times 1.3^\circ$
UKESM2-0-LL	1	National Institute of Meteorological Sciences/Korea Meteorological Administration (KOR)	$1.9^\circ \times 1.3^\circ$

Models in bold were selected for the “cold Tibetan-Plateau” composite